Effects of Vertical Eddy Diffusivity Parameterization on the Evolution of Landfalling Hurricanes

FEIMIN ZHANG

College of Atmospheric Sciences, Lanzhou University, Lanzhou, China, and Department of Atmospheric Sciences, University of Utah, Salt Lake City, Utah

ZHAOXIA PU

Department of Atmospheric Sciences, University of Utah, Salt Lake City, Utah

(Manuscript received 21 July 2016, in final form 10 March 2017)

ABSTRACT

As a result of rapid changes in surface conditions when a landfalling hurricane moves from ocean to land, interactions between the hurricane and surface heat and moisture fluxes become essential components of its evolution and dissipation. With a research version of the Hurricane Weather Research and Forecasting Model (HWRF), this study examines the effects of the vertical eddy diffusivity in the boundary layer on the evolution of three landfalling hurricanes (Dennis, Katrina, and Rita in 2005).

Specifically, the parameterization scheme of eddy diffusivity for momentum K_m is adjusted with the modification of the mixed-layer velocity scale in HWRF for both stable and unstable conditions. Results show that the change in the K_m parameter leads to improved simulations of hurricane track, intensity, and quantitative precipitation against observations during and after landfall, compared to the simulations with the original K_m.

Further diagnosis shows that, compared to original K_m, the modified K_m produces stronger vertical mixing in the hurricane boundary layer over land, which tends to stabilize the hurricane boundary layer. Consequently, the simulated landfalling hurricanes attenuate effectively with the modified K_m, while they mostly inherit their characteristics over the ocean and decay inefficiently with the original K_m.

1. Introduction

Landfalling hurricanes are a significant weather-related threat both onshore and inland. They cause great loss as a result of their strong winds, heavy rainfall, soil erosion, and flooding (Wu and Kuo 1999; Kaplan and DeMaria 2001; Whitehead 2003). Accurate prediction of the track, intensity, and structure associated with the weakening of hurricanes during landfall and their further evolution over land is of great interest in order to provide effective warning. Yet this is a great challenge and a key scientific issue for numerical weather prediction (NWP) (Marks and Shay 1998; Pu et al. 2009; Wu et al. 2016). Understanding the evolution of landfalling hurricanes is very important for improving their forecasts.

When a hurricane moves from ocean to land, the environmental conditions change significantly. Interaction between the hurricane and the environment over land becomes very important for the evolution of the hurricane. In the early 1980s, the Hurricane Strike Project was launched to gain some understanding of hurricane landfall. Results from Powell (1982, 1987) showed that the loss of the oceanic heat and moisture source, combined with the advection of drier air on the landward side of the storm, was responsible for cooling and drying the inflowing boundary layer air. In addition, the asymmetric structure of the surface wind field was caused by the combined effects of land–sea roughness differences, background environmental flow, and storm translation. Observation results from Powell (1990) confirmed that convective downdrafts are capable of transporting low–equivalent potential temperature (θ_e) air to the surface, where the mixed layer is eliminated. The incorporation of this air into the convection near the core of the storm may weaken the storm, depending on the scale of the disturbance and the processes governing the recovery of the air while it is flowing toward the eyewall. Simulation

Corresponding author: Dr. Zhaoxia Pu, zhaoxia.pu@utah.edu

Publisher's Note: This article was revised on 26 May 2017 to correct the spelling of the first author's name.

DOI: 10.1175/JAS-D-16-0214.1

results of Hurricane Danny (1997) by Kimball (2006) further emphasized that the erosion of the rainband convection and the approach of dry air to the storm core from the landward side could be the mechanism that reduces hurricane intensity.

Although the aforementioned studies led to significant understanding of hurricane landfalls, most of them, as well as some follow-on studies (e.g., Powell and Houston 1996; Farfán and Zehnder 2001), focused mainly on the near-landfall periods when hurricanes were not far from the ocean and were strongly influenced by oceanic effects. So far, very few studies have documented the evolution, intensity changes, thermodynamic characteristics, and precipitation features of hurricanes over land, although the mesoscale wind and precipitation structures of a hurricane over inland areas can cause the heaviest damage (Parrish et al. 1982; Bluestein and Hazen 1989).

During the evolution of a hurricane, the exchange and translation of momentum, heat, moisture, and substance between hurricanes and the surface/environment are significantly related to the planetary boundary layer (PBL). Past studies (e.g., Emanuel 1995; Braun and Tao 2000; Bao et al. 2002; Chen et al. 2007) have revealed that simulated hurricane intensity is quite sensitive to the exchange with enthalpy (heat and moisture) fluxes from the ocean surface. The importance of the interactions between the surface and PBL is also highlighted by recent studies (e.g., Zhu 2008; Zhu and Furst 2013; Doyle et al. 2014). In the NWP model, the PBL scheme is responsible for vertical subgrid-scale fluxes because of eddy transports throughout the atmosphere and is also closely related to cloud physics. Li and Pu (2008) evaluated the early rapid intensification of Hurricane Emily (2005) over the ocean with different PBL and cloud microphysical schemes, finding that high-θ_e air feeding from the ocean surface into the hurricane eyewall was evident in more enhanced convection and intense storms. Shelton and Molinari (2009) found that abnormally dry air upshear, together with cold downdrafts, might be responsible for the weakening of hurricanes over the ocean. Nolan et al. (2009a,b) evaluated the Yonsei University (YSU) and Mellor–Yamada–Janjić (MYJ) PBL schemes in an advanced research version of the Weather Research and Forecasting (WRF; Skamarock et al. 2008) Model using in situ data obtained from aircraft. Results show that, for both schemes, the differences between the low-level asymmetries in the simulated and observed wind fields over the ocean appear to be related to eyewall asymmetries forced by environmental wind shear. Riemer et al. (2010) and Cione et al. (2013) also indicated that the low-level dry air (low-θ_e air) contributes to hurricane evolution over the ocean and that the transport of dry air within the PBL is important to hurricane decay. Zhang et al. (2013) investigated the asymmetric structure of the hurricane PBL in relation to the environmental vertical wind shear in the inner-core region, based on observations over the ocean, and the results suggest that the convective downdraft and the θ_e transport within the PBL are different in the four quadrants of the hurricane vortex. Zhu et al. (2014) evaluated the effects of four PBL schemes in the WRF Model on the simulation of Hurricane Isabel (2003) over the ocean. The results showed that the vertical transport of surface heat and moisture is critical to storm structures in the vicinity of the hurricane eyewall.

As key parameters in PBL parameterization, eddy diffusivity for momentum K_m and thermal eddy diffusivity K_h control the feedback of momentum, moisture, and heat between the surface and the atmosphere. A series of numerical and observational studies has been conducted by various groups for hurricanes over the ocean. For instance, Kepert (2001), Smith (2003), and Zhang et al. (2011) found that better estimations of the eddy diffusivity coefficient in the hurricane boundary layer are helpful for hurricane prediction over the ocean. Braun and Tao (2000) investigated the sensitivity of numerical simulations of a hurricane to different PBL schemes in the fifth-generation Pennsylvania State University–NCAR Mesoscale Model (MM5), finding that the simulated intensity was related to the vertical mixing in each PBL scheme over the ocean, especially for the Medium-Range Forecast (MRF) scheme. Zhang and Drennan (2012) estimated the vertical distribution of vertical eddy diffusivities over the ocean through observation. They found that the magnitudes of vertical eddy diffusivities for momentum and latent heat fluxes were comparable, but the eddy diffusivity for sensible heat flux was much smaller than that for latent heat flux. Gopalakrishnan et al. (2013) artificially reduced eddy diffusivity to a quarter of its original value in the Hurricane Weather Research and Forecasting Model (HWRF) and produced the intensity and size of a hurricane best matched with observations when it was over the ocean, indicating the importance of eddy diffusivity in PBL parameterization. Zhang et al. (2015) reduced K_m with $\alpha = 0.5$ in HWRF. Results with four hurricanes over the ocean showed that predictions were improved with a smaller K_m. Compared to simulations with the original K_m, the simulated storms were stronger and had a shallower PBL, stronger inflow and outflow above the PBL, stronger updrafts in the eyewall, and a stronger warm core.

Overall, as mentioned above, the importance of PBL parameterization and the effects of vertical mixing (determined by vertical K_m and K_h) in the hurricane boundary layer has been frequently investigated because of the strong effect on simulated hurricane intensity and structure. However, these findings and improvements are limited mostly to when hurricanes are over the ocean. So far, to the best of our knowledge, similar research for hurricanes over

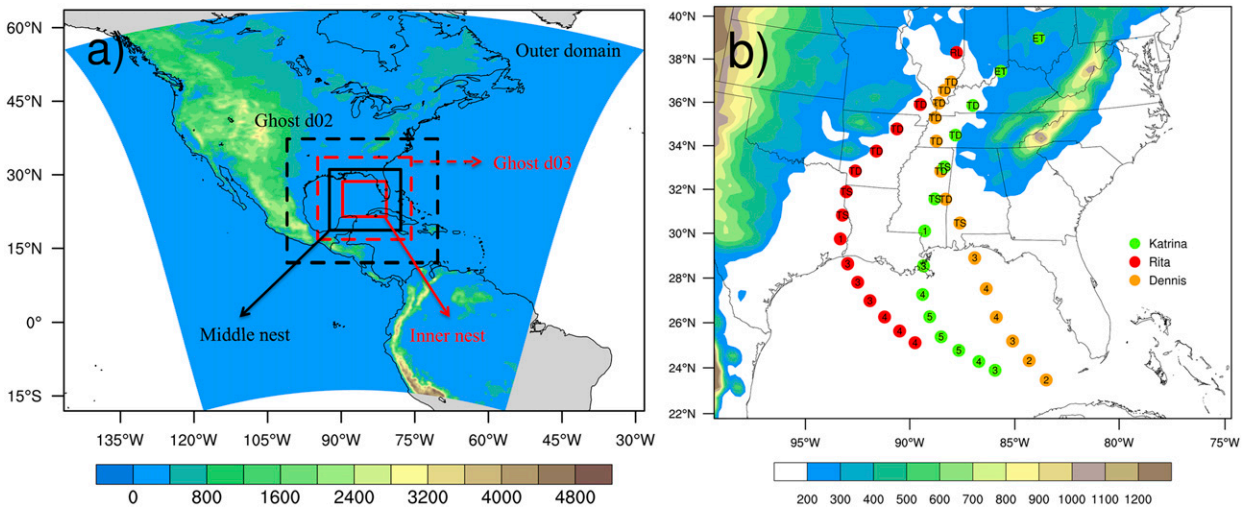

FIG. 1. (a) Locations of HWRF domains. The simulation is performed in outer, middle, and inner domains. The middle and inner domains move with the simulated hurricane. Two ghost domains are used for HWRF initialization purposes only. (b) Best-track positions at 6-h intervals for Hurricane Dennis from 1200 UTC 9 Jul to 1800 UTC 12 Jul 2005, Hurricane Katrina from 0000 UTC 28 Aug to 0600 UTC 31 Aug 2005, and Hurricane Rita from 0000 UTC 23 Sep to 0600 UTC 26 Sep 2005. The symbols in the circle indicate the hurricane intensity scales, from NHC and derived by Saffir–Simpson category: tropical storm (TS), tropical depression (TD), remnant low (RL), and extratropical (ET). The shaded contours indicate the terrain height (m). Contour intervals are different in (a) and (b). The ghost domain in (a) is created for inner-core data assimilation; the domain sizes for ghost d02 and ghost d03 are 20° × 20° and 10° × 10°, respectively.

land has not yet been documented. Understanding of the kinematic and thermal structures during hurricane landfall and their further evolution over land is generally lacking, as the changes in hurricane boundary layer structures and the interaction between hurricanes and surface conditions can be significantly different over the ocean and land.

In light of the lack of studies on the interactions between the hurricane boundary layer and the land surface/environment, as well as the poor understanding of hurricane evolution over land, the purpose of this study is to investigate the effects of vertical mixing in the PBL on landfalling hurricanes, with the emphasis on hurricanes over land, based on a research version of the National Centers for Environmental Prediction (NCEP)'s HWRF (version 3.6a; Tallapragada et al. 2014). The detailed thermodynamic and kinematic characteristics of hurricanes during their movement from ocean to land as well as their evolution and decay processes over land are diagnosed.

The paper is divided into the following sections. Section 2 gives a brief description of the three hurricane cases, the data, and HWRF. The PBL parameterization and the proposed modification of the vertical eddy diffusivity parameterizations are presented in section 3. Section 4 presents the simulation results of Hurricane Rita (2005), Hurricane Katrina (2005), and Hurricane Dennis (2005), as well as the discussions of the effects of vertical mixing in the PBL on hurricane thermodynamic and kinematic structures. The discussion and concluding remarks are made in sections 5 and 6, respectively.

2. Description of hurricane cases, data, and HWRF

The 2005 hurricane season had a total of five named storms that made landfall in the Gulf of Mexico, which is one of the regions where hurricanes most frequently make landfall in the Atlantic basin (Brettschneider 2008). Among them, three hurricanes—Dennis (Beven 2005), Katrina (Knabb et al. 2005), and Rita (Knabb et al. 2006)—are the representative landfalling hurricanes because of their damage, loss of life, severe weather, and floods caused by storm surges. Hurricanes Dennis, Katrina, and Rita made landfall at 1930 UTC 10 July, 1110 UTC 29 August, and 0740 UTC 24 September, respectively.

These three hurricanes were chosen because they all strengthened to a category-4–5 hurricane (on the Saffir–Simpson hurricane wind scale) in the central Gulf of Mexico and weakened prior to making landfall as a category-3 hurricane (Fig. 1b). They also resulted in severe destruction and had long-term duration over land.

Considering data availability and the major emphasis of this study, we chose the following time periods for numerical simulation: from 1200 UTC 9 July to 1800 UTC 12 July 2005 for Hurricane Dennis, from 0000 UTC 28 August to 0600 UTC 31 August 2005 for Hurricane Katrina, and from 0000 UTC 23 September to 0600 UTC 26 September 2005 for Hurricane Rita, when these tropical cyclones (TCs) all underwent intensity changes following an initial rating of strong category-4–5 hurricanes, a slow weakening to category 3, and deep weakening to

tropical storms and tropical depressions near, during, and after their landfalls.

HWRF has been an operational model implemented at NCEP to provide numerical guidance to the National Hurricane Center (NHC) for the forecast of the track, intensity, and structure of TCs since 2007. More importantly, it has also become a popular and reliable model for hurricane research owing to its encouraging success in forecasting hurricanes and significant improvements in its forecast score during recent hurricane seasons. At the beginning of this study, HWRF, version 3.6, released by the NCAR Developmental Testbed Center (DTC) became available and was thus adopted for this study. HWRF has a Nonhydrostatic Mesoscale Model (NMM) dynamic core (Janjić et al. 2010) with a two-way interactive, movable, triple-nested grid procedure. The three domains are at horizontal grid resolutions of 27, 9, and 3 km that cover areas of roughly 80° × 80°, 12° × 12°, and 7.1° × 7.1°, respectively. Figure 1a shows the configuration of the simulation domain. Detailed physical parameterization schemes, forcing data, and dynamic structures can be found in the HWRF scientific documentation (Tallapragada et al. 2014).

The NCEP Global Forecasting System (GFS) Final Analysis (FNL) data (1° × 1°) are used for the initial and boundary conditions in a cold-start mode. The vortex initialization scheme (Liu et al. 2006) was performed to relocate the hurricane vortex at the location determined by the NHC Tropical Cyclone vital statistics (TCVitals), then followed by a size and intensity correction process with adjustments to the wind, moisture, and thermodynamics fields. The ocean model (Mellor 2004) is not included in this study.

Satellite infrared imagery from the *Geostationary Operational Environmental Satellite 12* (*GOES-12*); NHC best-track data and surface wind analysis from the Hurricane Research Division (HRD); and precipitation analysis from the NCEP Climatology Calibrated Precipitation Analysis (CCPA) reanalysis (Hou et al. 2014) are used for validating the simulation results.

3. Modifying vertical eddy diffusivity in PBL parameterization

The PBL scheme used in HWRF (called the GFS scheme) is essentially the traditional NCEP MRF scheme, which is a first-order nonlocal scheme (Troen and Mahrt 1986; Hong and Pan 1996):

$$\frac{\partial C}{\partial t} = \frac{\partial}{\partial z}\left[K_c\left(\frac{\partial C}{\partial z}\right) - \gamma_c\right], \tag{1}$$

where C is the prognostic mean variable (such as u, v, θ, q); and γ_c represents the nonlocal term of C. The eddy diffusivity is K_c, and we denote K_m as the momentum eddy diffusivity for u and v and K_h as the thermal eddy diffusivity for θ and q.

In HWRF, K_m is parameterized as:

$$K_m = kw_s z\left[\alpha\left(1-\frac{z}{h}\right)^p\right] \quad \text{and} \tag{2}$$

$$w_s = \frac{u_*}{\phi_m}, \tag{3}$$

where $k = 0.4$ is the von Kármán constant; w_s represents the mixed-layer velocity scale; u_* is the surface frictional velocity that relates to wind shear or momentum fluxes near the ground (Stull 1988); h is the depth of the turbulent PBL [viz., the PBL height (PBLH)], which is determined based on the height above the ground at which the bulk Richardson number R_{ib} exceeds a critical value; ϕ_m is the dimensionless wind profile function evaluated at the top of the surface layer ($z = 0.1h$), which can be parameterized by the Monin–Obukhov scale that relates to both surface momentum and heat and moisture fluxes (Stull 1988; Hong and Pan 1996); z is the height above the surface; p is the profile-shape exponent, taken to be 2.0 in HWRF; and α is the nonzero constant ($\alpha = 0.7$ in HWRF 3.6a; same as the 2013 version HWRF) to reduce the magnitude of K_m as proposed by Zhang et al. (2012) and Gopalakrishnan et al. (2013). In HWRF, the parameterization of w_s [Eq. (3)] is used under both stable and unstable stratifications.

In the GFS scheme, K_h is parameterized as follows:

$$K_h = \frac{K_m}{P_r} \quad \text{and} \tag{4}$$

$$P_r = \frac{\phi_h}{\phi_m} + \varepsilon bk, \tag{5}$$

where ϕ_h/ϕ_m is the ratio of the dimensionless temperature gradient and wind profile at the top of the surface layer ($z = 0.1h$); $k = 0.4$ is the von Kármán constant; and ε and b are constants, taken to be 7.8 and 0.1, respectively. Thus, the Prandtl number P_r is a constant in the whole PBL under certain stability.

So far, improvements of PBL parameterization in HWRF have focused mainly on K_m, using the nonzero constant ($\alpha = 1$) to cap the unrealistic strong vertical mixing in the PBL based on ocean field experiments. This method has been proved to be very useful for improving hurricane prediction over the ocean (Gopalakrishnan et al. 2013; Zhang et al. 2012, 2015); however, very few have focused on sensitivity studies or possible impacts of vertical eddy diffusivity parameterization on hurricane evolution during and after landfall.

During the previous development of the MRF scheme, the convective velocity scale w_{*b} [see Eq. (7)],

which is an important scaling variable in PBL that consists of the surface buoyancy flux [denoted as $(g/\overline{\theta_{va}})\overline{(w'\theta'_v)}_0$] and the boundary layer height, is adopted from Noh et al. (2003) to parameterize vertical eddy diffusivity in PBL. This term works quite well when the magnitude of the vertical velocity fluctuation in thermals is on the same order as w_{*b} [e.g., convective boundary layer (Stull 1988)]. Combined with other modifications, such as the Prandtl number and entrainment, the modified scheme produces profiles that are more realistic when compared to the data from large-eddy simulations. The real case study by Hong et al. (2006) also showed that the new scheme portrayed the characteristics of intense inland convection systems well. Moreover, these modifications have also been conducted and applied in the well-known YSU scheme (Hong et al. 2006). In light of these results, we examine the sensitivity of the modification that relates to K_m to the simulation of landfall hurricanes with HWRF, based on Stull (1988), Noh et al. (2003), and Hong et al. (2006).

The modification is the mixed-layer velocity scale w_s to adjust K_m:

$$w_s = \left(u_*^3 + \phi_m k w_{*b}^3 \frac{z}{h}\right)^{1/3}, \tag{6}$$

while

$$w_{*b} = \left[\frac{gh}{\overline{\theta_{va}}}\overline{(w'\theta'_v)}_0\right]^{1/3}, \tag{7}$$

where w_{*b} is the convective velocity scale for moist air; g denotes gravity acceleration; $\overline{\theta_{va}}$ is the virtual potential temperature at the lowest model level; and $\overline{(w'\theta'_v)}_0$ represents the surface heat and moisture fluxes. Other symbols have been introduced above. Considering the surface and atmosphere interaction is stronger than usual cases during the hurricane landfall even in a quasi-stable atmospheric condition, note here w_s [Eq. (6)] is used for both stable and unstable stratifications. This is different from the YSU scheme because w_s is termed as Eq. (3) under stable stratification only in the YSU scheme.

Overall, the above modifications are essentially the parameterization of w_s for K_m in the PBL parameterization, without any others modifications of HWRF.

A surface-layer scheme is coupled with the PBL scheme. HWRF uses a modified Geophysical Fluid Dynamics Laboratory (GFDL) surface-layer parameterization based on the Monin–Obukhov similarity theory (Sirutis and Miyakoda 1990; Kurihara and Tuleya 1974). Details can be found in Tallapragada et al. (2014).

TABLE 1. Parameterization configurations in each experiment.

Expt	Stable conditions	Unstable conditions
CTL	$w_s = \dfrac{u_*}{\phi_m}$	$w_s = \dfrac{u_*}{\phi_m}$
REV1	$w_s = \left(u_*^3 + \phi_m k w_{*b}^3 \dfrac{z}{h}\right)^{1/3}$	$w_s = \left(u_*^3 + \phi_m k w_{*b}^3 \dfrac{z}{h}\right)^{1/3}$
REV2	$w_s = \dfrac{u_*}{\phi_m}$	$w_s = \left(u_*^3 + \phi_m k w_{*b}^3 \dfrac{z}{h}\right)^{1/3}$

4. Simulation results

To examine the effects of the modified K_m on hurricane simulations, at the beginning of the study, two experiments are conducted for each of the three hurricane cases:

1) CTL: the original HWRF without any modification;
2) REV1: K_m only is modified and used in both stable and unstable conditions, while the form of K_h remains the same as in CTL.

The detailed configurations of the two experiments are also summarized in Table 1.

For each experiment, three time periods are defined to represent the evolution of the hurricanes from ocean to land: prelandfall, when the hurricane is over the ocean (before 36-h forecast); landfall (near 36-h forecast), defined as the time when the hurricane center crosses the coastline; and postlandfall, when the hurricane travels over land (beyond 36-h forecast).

a. Track and intensity

Figures 2 and 3 compare the HWRF simulations of track and intensity with the NHC best-track data for all three hurricanes in different experiments. Over the ocean, in the early forecasting phase, simulation results from the other experiments are similar to those of CTL. Near and over land, however, the impact of the modification of K_m on hurricane track and intensity simulations is evident. While much stronger hurricanes with overestimated surface wind and underestimated surface pressure (against the best-track data) are produced by the original HWRF (CTL), noticeable improvements in track and intensity simulations are found in REV1. The large track error in CTL is also improved in REV1 (Figs. 3a,d,g). Overall, the decay processes of hurricanes after their landfalls are much underestimated by the simulations with the original scheme, but they are well portrayed with the modified K_m. In addition, a comparison of the simulated track positions among the experiments in Fig. 2 also shows that the unrealistic track positions in CTL are ably remedied by REV1. Compared with CTL, the mean improvements during hurricane evolution over land due to the modification of K_m

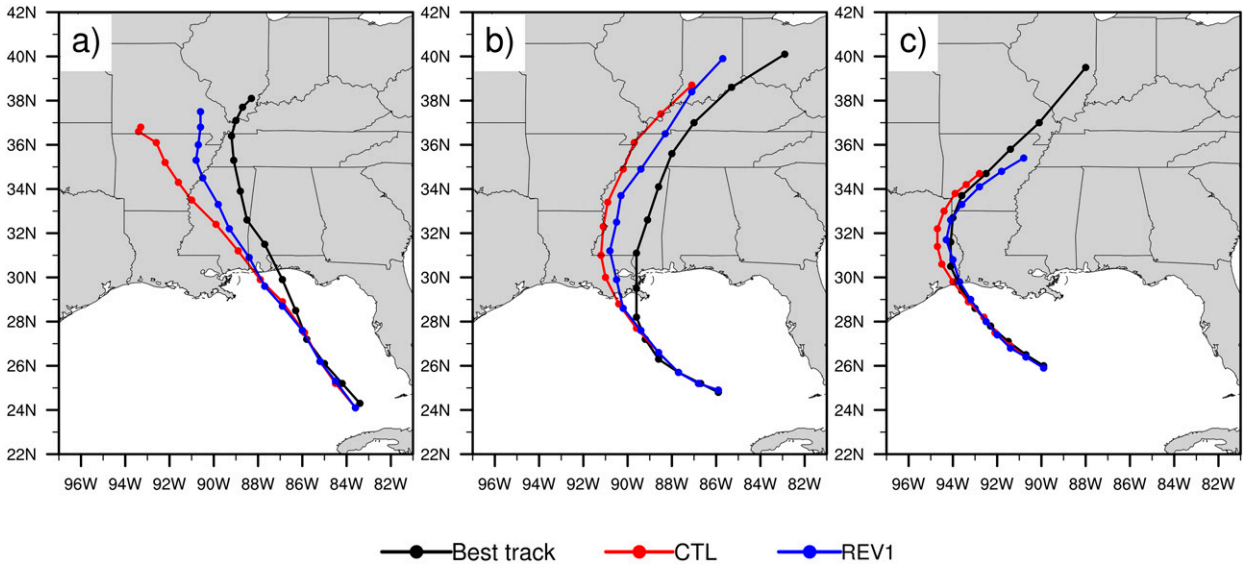

FIG. 2. Comparison of hurricane track positions between NHC best-track and different simulation experiments at 6-h intervals. (a) Hurricane Dennis from 1200 UTC 9 Jul to 1800 UTC 12 Jul 2005, (b) Hurricane Katrina from 0000 UTC 28 Aug to 0600 UTC 31 Aug 2005, and (c) Hurricane Rita from 0000 UTC 23 Sep to 0600 UTC 26 Sep 2005.

for track, minimum surface pressure, and maximum surface wind are about ~87 km, ~12 hPa, and ~7.5 m s^{-1}, respectively, for Hurricane Rita; ~95 km, 11 hPa, and ~0.5 m s^{-1}, respectively, for Hurricane Katrina; and ~141 km, ~4 hPa, and ~3.7 m s^{-1}, respectively, for Hurricane Dennis. The simulated landfall time is different than best track and does not essentially affect the main conclusion (Nolan et al. 2009a).

Because of the similarities regarding the impacts of the modified K_m on all hurricanes, most of the diagnosis results are presented for Hurricane Rita.

b. *Evolution of hurricanes and synoptic environments*

Figures 4a–e and 4f–j show the GOES IR imagery for Rita and Katrina, respectively. When hurricanes are located over the ocean (Figs. 4a,f), the symmetrical convective spiral bands and hurricane eye are clearly evident. Intense convection covers most of the hurricane core regions and outer rainbands with very high cloud tops, indicating strongly organized hurricane structure. During and right after landfall (Figs. 4b,c,g,h), the symmetrical features of the spiral bands and the presence of the hurricane eye are no longer evident. The hurricanes are obviously weakened, with decreased cloud tops and convective regions, especially north of the eyewalls, implying environmental infusion effects over land. When hurricanes further evolve over land, the cloud tops become lower and convective spiral bands become looser, with asymmetric convective structures, especially along the hurricane center (Figs. 4d,i). Then the spiral structure of the storms gradually weakens and eventually dissipates (Figs. 4e,j).

Figures 5a–d and 5e–h compare the NCEP FNL and simulated geopotential height and temperature fields valid at 0600 UTC 26 September 2005 and 0600 UTC 31 August 2005 for Hurricanes Rita and Katrina, respectively. The overall large-scale synoptic characteristics from the West Coast to East Coast are well captured by HWRF simulations in both CTLs and REV1s. Specifically, the great differences between CTLs and REV1s are mainly over the environmental flows around and associated with the hurricane vortices (Figs. 5d,h). In Hurricane Katrina, for example, to the east of the Great Plains, CTL predicts a stronger trough (Fig. 5f) compared to FNL (Fig. 5e) with closed low pressure, while REV1s produce a trough (Fig. 5g) without the closed structure that is compatible with FNL. Figures 5d and 5h also show the differences in mean wind fields (i.e., 850–300 hPa) between CTL and REV1 (CTL minus REV1). They reveal that the flow differences between the two experiments are obvious over the areas around and associated with the hurricane vortices, where the simulated winds in CTLs are stronger with more spiral structures than those in REV1s. Specifically, the difference in the maximum wind between CTL and REV1 also indicate that the flow direction in CTL is more northwesterly, which is opposite of the best-track direction (as shown in Fig. 2). Therefore, the unrealistic spiral environmental flows around and associated with hurricane vortices given by CTL are responsible for the larger bias in the track simulations compared with REV1.

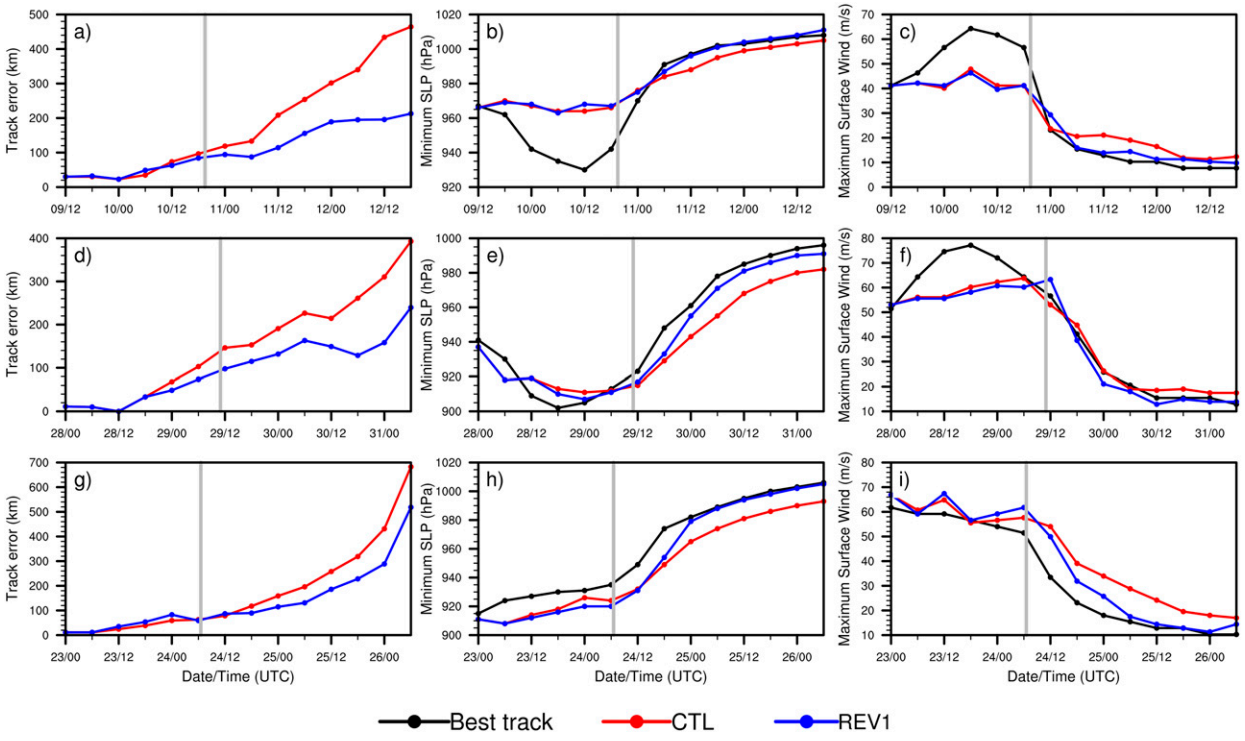

FIG. 3. Time series of (a),(d),(g) track errors (km) and intensity in terms of (b),(e),(h) minimum central SLP (hPa) and (c),(f),(i) maximum surface wind ($m\,s^{-1}$) at 6-h intervals against NHC best-track data from different experiments for (a)–(c) Hurricane Dennis from 1200 UTC 9 Jul to 1800 UTC 12 Jul 2005, (d)–(f) Hurricane Katrina from 0000 UTC 28 Aug to 0600 UTC 31 Aug 2005, and (g)–(i) Hurricane Rita from 0000 UTC 23 Sep to 0600 UTC 26 Sep. The solid gray line denotes the approximate hurricane landfall time.

The evolution of sea level pressure (SLP) fields (Fig. 6) for both Rita (left) and Katrina (right) further indicates that CTLs predict stronger hurricanes with stronger SLP gradients compared with REV1s when hurricanes interact with the land surface, implying a slower decay process in CTLs after landfall. In contrast, REV1s make the vortex decay process more efficient after the hurricane makes landfall.

c. *Precipitation*

Quantitative precipitation forecasts (QPFs) for hurricanes are very important for improving the prediction of inland flooding (Elsberry 2002). Accumulated precipitation was checked for all three hurricanes during their landfalls (Fig. 7). With the original HWRF, all CTL experiments tend to overestimate rainfall for all three hurricanes, when compared with the NCEP CCPA data, a finescale and high-quality precipitation analysis that is used at NCEP for forecast verification. With the modified K_m (experiment REV1s), however, the overestimations of precipitation amounts are mitigated, and the simulations produce more reasonable precipitation structures for all three hurricanes. For instance, Figs. 7a–c show that the overestimated precipitation and missing rainfall over southeastern Missouri in CTL are remedied in REV1 for the simulation of Hurricane Dennis. Figures 7d–f indicate that precipitation of Hurricane Katrina produced by REV1 is closer to CCPA, compared to CTL. The modified K_m also leads to an improved precipitation structure against CCPA by remedying the much stronger rainfall in CTL during the simulation of Hurricane Rita (Figs. 7g–i). In addition, the rainfall to the northeast of Rita that is missed by CTL is also well simulated by REV1 with the modified K_m.

Equitable threat scores (ETSs) (Wilks 1995) were calculated for all three cases for the 24- and 42-h accumulated precipitation for the periods after the hurricanes made landfall, against the NCEP CCPA data. Results in Fig. 8 show clearly that all experiments with modified K_m (REV1) lead to a better ETS, compared with CTL, especially for light rainfall (less than 40 mm). The improved QPFs and rainfall structures could be attributed to the improved track simulations (Fig. 2) and better representation of convective structures (discussed in section 5) by the modified K_m.

d. *Effects on vortex structure*

The simulation results above have shown that the original HWRF parameterization tends to produce hurricanes

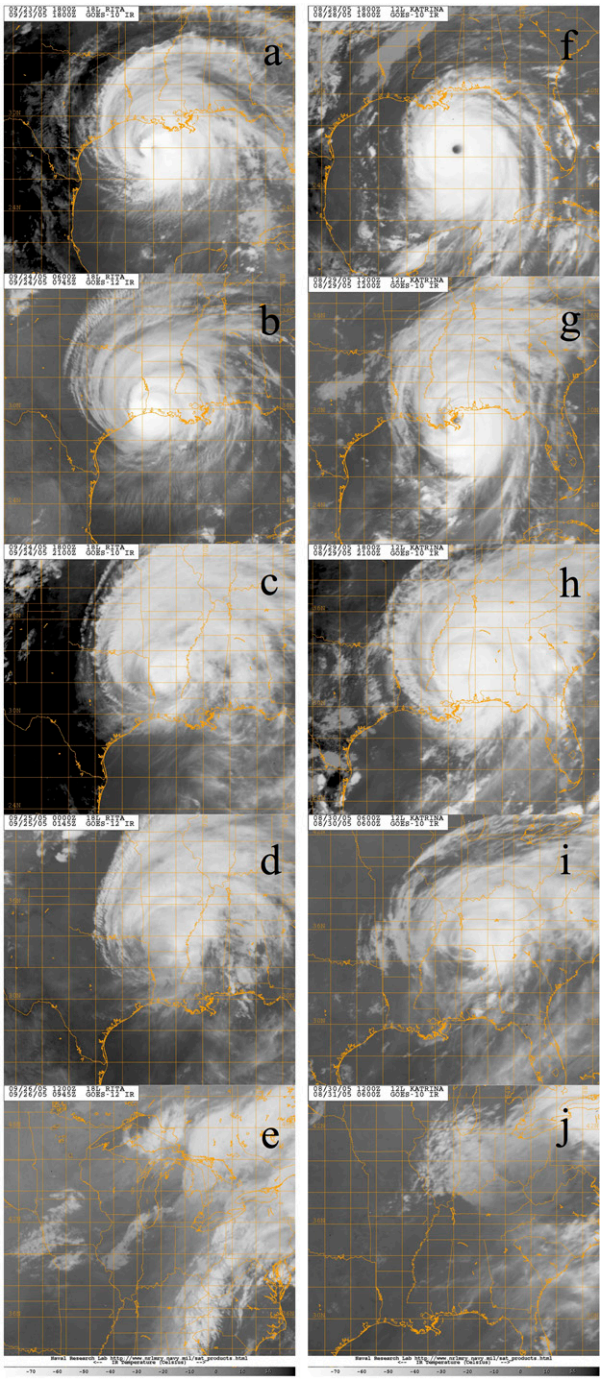

FIG. 4. GOES infrared imagery during hurricane evolution from ocean to land, corresponding to (a),(f) 18-; (b),(g) 36-; (c),(h) 45-; (d),(i) 54-; and (e),(j) 78-h forecasts for (a)–(e) Hurricane Rita and (f)–(j) Hurricane Katrina. The initial time is 0000 UTC 23 Sep 2005 for Hurricane Rita and 0000 UTC 28 Aug 2005 for Hurricane Katrina. [Courtesy of the Naval Research Laboratory TC website (http://www.nrlmry.navy.mil/tc_pages/tc_home.html).]

with overestimated intensity, rainfall, and spiral vortices during their landfall, but the modified K_m has evident positive impacts on the simulation of the decay process of hurricane vortices during and after their landfall. In fact, landfalling hurricanes have direct interactions with the land surface beneath them. When a hurricane makes landfall, the immediate interface beneath it changes from ocean to land. Thus, the thermodynamic conditions beneath it should change significantly because of ocean and land contrasts. Figure 9 illustrates the azimuthally averaged surface sensible heat fluxes, latent heat fluxes, and total enthalpy fluxes during the evolution of Rita from ocean to land, respectively. Results from both CTL and REV1 experiments show that, when the hurricane moves from ocean to land, surface sensible (Figs. 9a,b) and latent fluxes (Figs. 9c,d) decrease dramatically beneath and around the vortices (i.e., with a radius of 0–300 km). Moreover, compared to CTL, the surface sensible heat fluxes decrease while the surface latent heat fluxes increase in REV1. The total enthalpy fluxes (Figs. 9e,f), however, are essentially the same in either CTL or REV1, indicating that the modification of K_m does not essentially change the pattern or strength of surface total enthalpy fluxes.

Figure 10 compares the evolution of azimuthally averaged K_m and K_h below 700 hPa in the CTL and REV1 schemes, respectively. Over the ocean, before hurricane landfall (Figs. 10a,f), the patterns of vertical mixing in the PBL are almost the same in the two experiments. However, vertical mixing in REV1 is slightly weaker than that in CTL. During and after landfall (Figs. 10b–e and 10g–j), when the hurricane interacts with the land surface directly, the vertical mixing in REV1 is more efficient than in CTL. In addition, vertical mixing in the PBL continues to decrease from ocean to land in the original parameterization, while it becomes most significant (K_m and K_h are at a maximum) at landfall time (Figs. 10b,g) with the modified K_m when the hurricane starts to interact with the land surface directly, suggesting that the modified parameterization has a great response to the rapid transition of surface boundary conditions when hurricanes move from ocean to land. Moreover, the pattern and the magnitude of K_m and K_h parameters are the same in either CTL or REV1, implying that vertical mixing in the PBL is determined mainly by the estimation of K_m parameter in HWRF, similar to the previous study (e.g., Hong and Pan 1996).

Comparisons of CTL and REV1 with respect to surface enthalpy fluxes (Fig. 9) and vertical mixing in the PBL (Fig. 10) indicate that noticeable interactions between hurricane vortices and the land surface in both original and modified schemes occur mainly around the hurricane vortices (i.e., 0–300-km radius from the hurricane center),

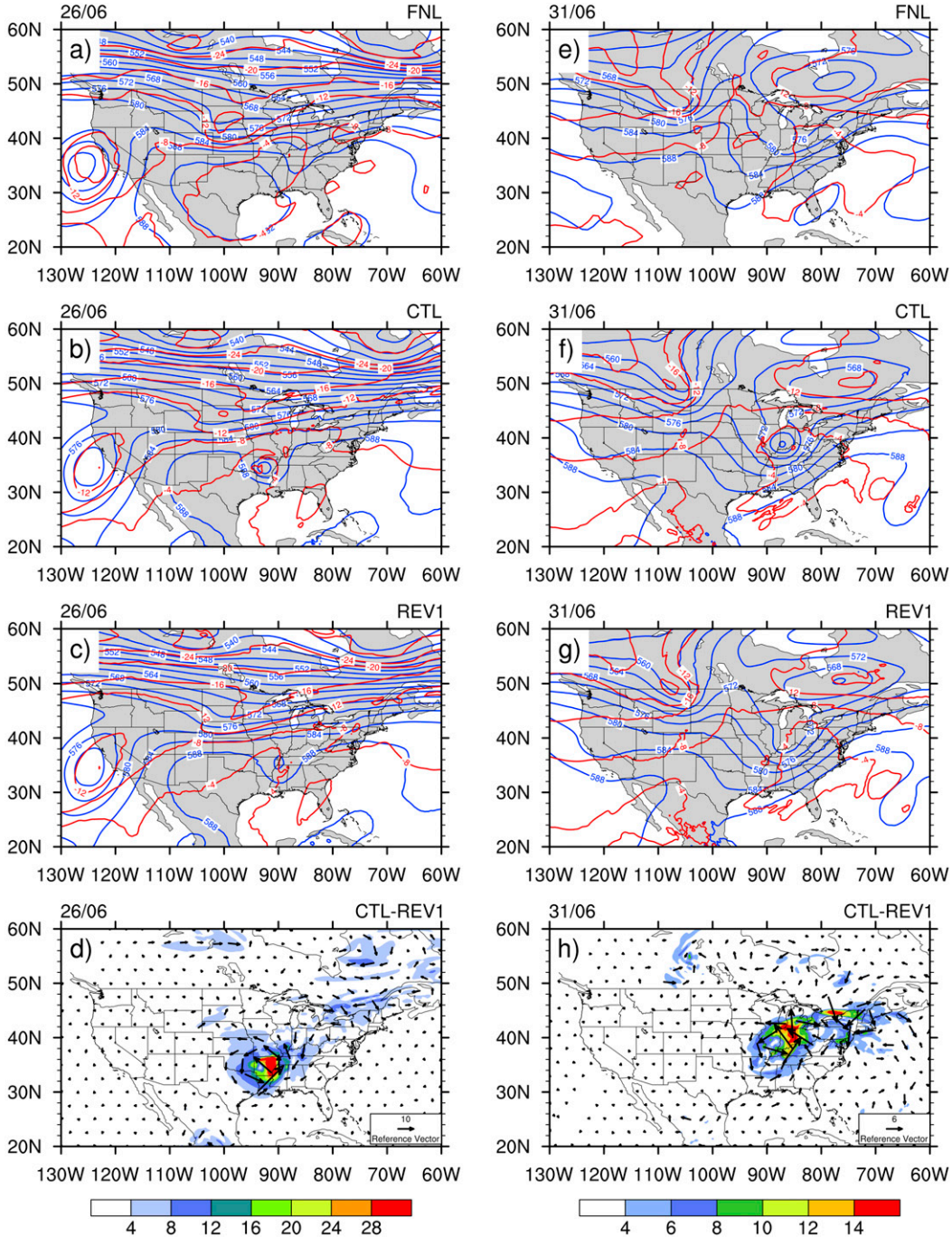

FIG. 5. Comparison of geopotential height (blue contour line; m) and temperature (red contour line; °C) among (a),(e) NCEP FNL, (b),(f) CTL, and (c),(g) REV1 at 500 hPa valid at 0600 UTC 26 Sep 2005 for (a)–(d) Hurricane Rita and 0600 UTC 31 Aug 2005 for (e)–(h) Hurricane Katrina. (bottom) The differences of mean wind vectors and speed (colored contours) from 850 to 300 hPa between CTL and REV1 (CTL minus REV1) for (d) Rita and (h) Katrina.

resulting in great discrepancies of flow around and associated with the hurricane vortices, as shown in Fig. 5.

Previous studies have revealed the important effects of the cold dry air from the environment around a hurricane's warm-core center on hurricane decay (Tuleya and Kurihara 1978; Powell 1987, 1990; Kimball 2006). Considering the great discrepancies in the vertical mixing between the original and modified PBL parameterizations, as well as the dramatically reduced land-surface enthalpy fluxes around and beneath the hurricanes

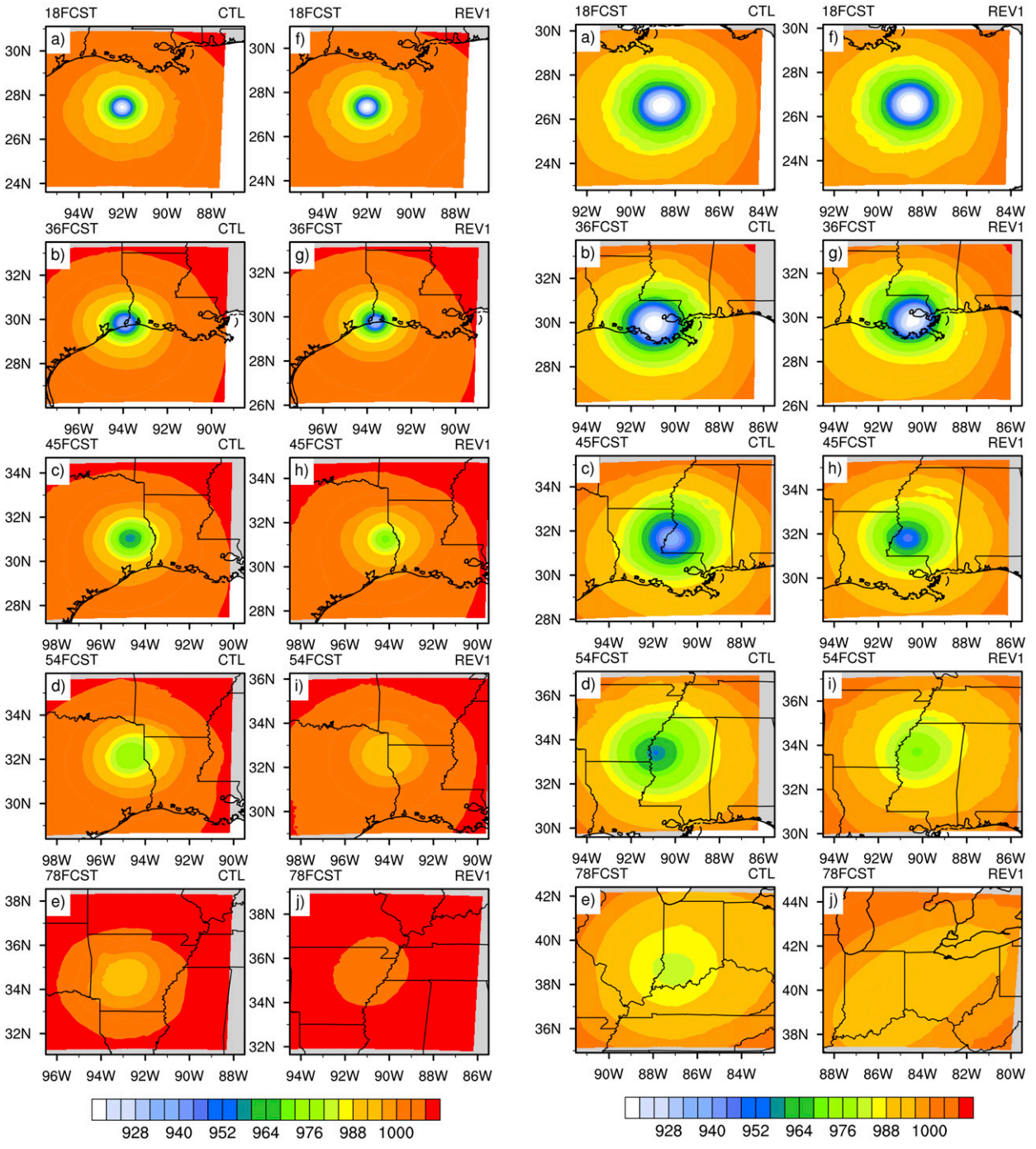

FIG. 6. Sea level pressure (hPa) during the evolution of (left two columns) Hurricane Rita and (right two columns) Hurricane Katrina from ocean to land at (a),(f) 18-; (b),(g) 36-; (c),(h) 45-; (d),(i) 54-; and (e),(j) 78-h forecasts, respectively. (a)–(e) CTL and (f)–(j) REV1. The initial time is 0000 UTC 23 Sep 2005 for Hurricane Rita and 0000 UTC 28 Aug 2005 for Hurricane Katrina.

(especially within a 0–300-km radius of the hurricane center), we further examine the effects of the modified K_m on the kinematic and thermodynamic structures of hurricane vortices within a radius of 300 km, which reflects the interaction between the hurricane's warm core and the associated environment before, during, and after its landfall.

Equivalent potential temperature θ_e represents the parcel properties in moist entropy processes. Higher θ_e means a parcel with high temperature and moisture

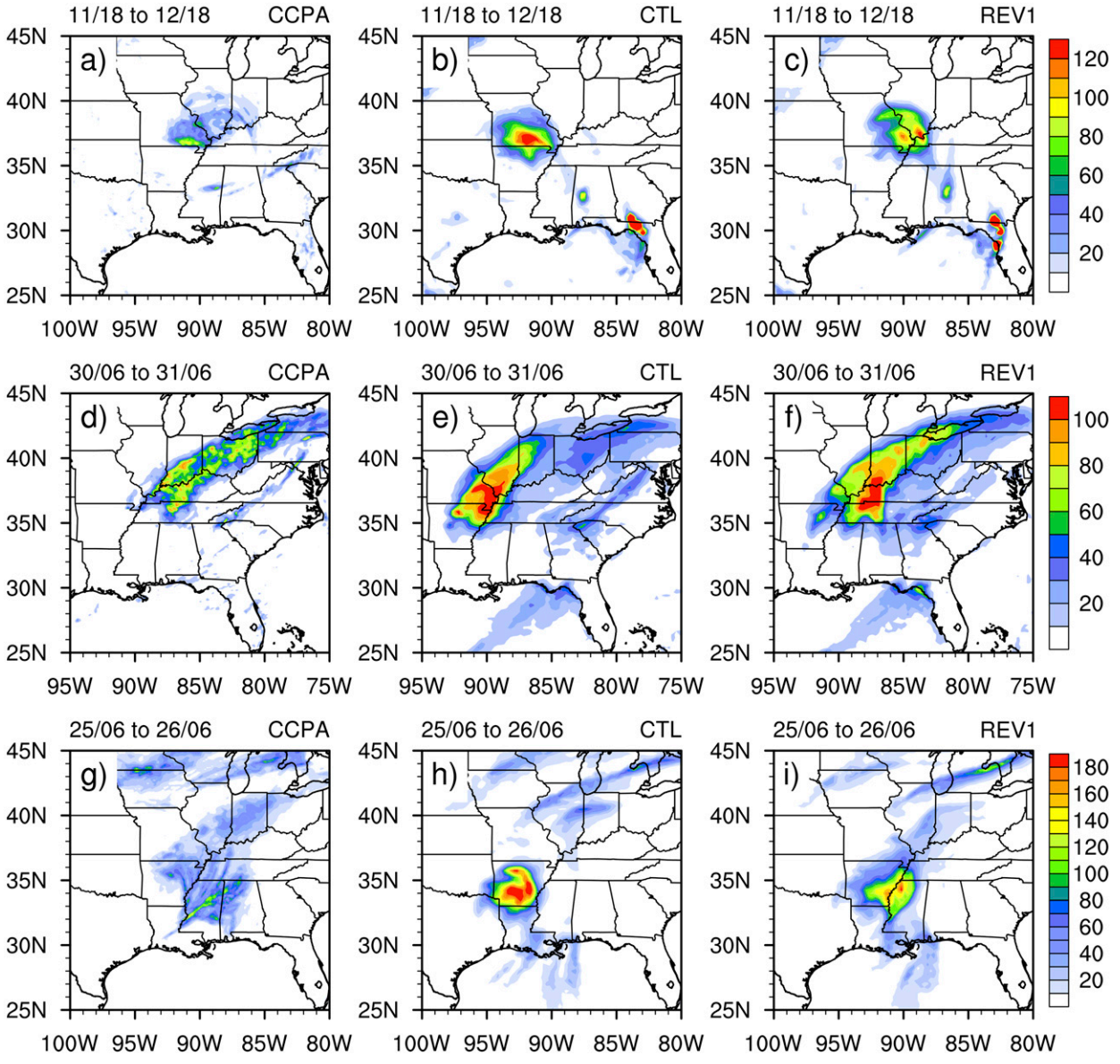

FIG. 7. Accumulated 24-h precipitation (mm) for (a)–(c) Hurricane Dennis, valid from 1800 UTC 11 Jul to 1800 UTC 12 Jul 2005; (d)–(f) Hurricane Katrina, valid from 0600 UTC 30 Aug to 0600 UTC 31 Aug 2005; (g)–(j) Hurricane Rita, valid from 0600 UTC 25 Sep to 0600 UTC 26 Sep. (a),(d),(g) CCPA; (b),(e),(h) CTL; and (c),(f),(i) REV1.

content, and vice versa. In addition, θ_e is also a useful tool for diagnosing the interactions between the warm core and the environment. For instance, Powell (1990) pointed out that the mechanisms that act to lower θ_e, if acting on large-enough scales to modify a significant portion of the inflowing boundary layer, would result in a cooling of the warm core and weakening of the storm. Figure 11 shows the azimuthally averaged θ_e and radial wind below 700 hPa. Strong contrasts are found in θ_e and radial wind before and after the hurricane made landfall. At the 18-h forecast, when the hurricane is over the ocean, θ_e and radial wind structures are quite similar and well represented in both CTL and REV1 (Figs. 11a,f). It seems that the warm-core θ_e and inflow/outflow are slight stronger in REV1 than that in CTL. This is due mainly to the slightly weaker vertical mixing in REV1 than that in CTL at this time (Figs. 10a,f), which tends to make the hurricane stronger over ocean (e.g., Gopalakrishnan et al. 2013; Zhang et al. 2015). During hurricane landfall at the 36-h forecast (Figs. 10b,g) in both CTL and REV1, the warm core becomes weaker than that at 18 h. Particularly, when hurricanes interact

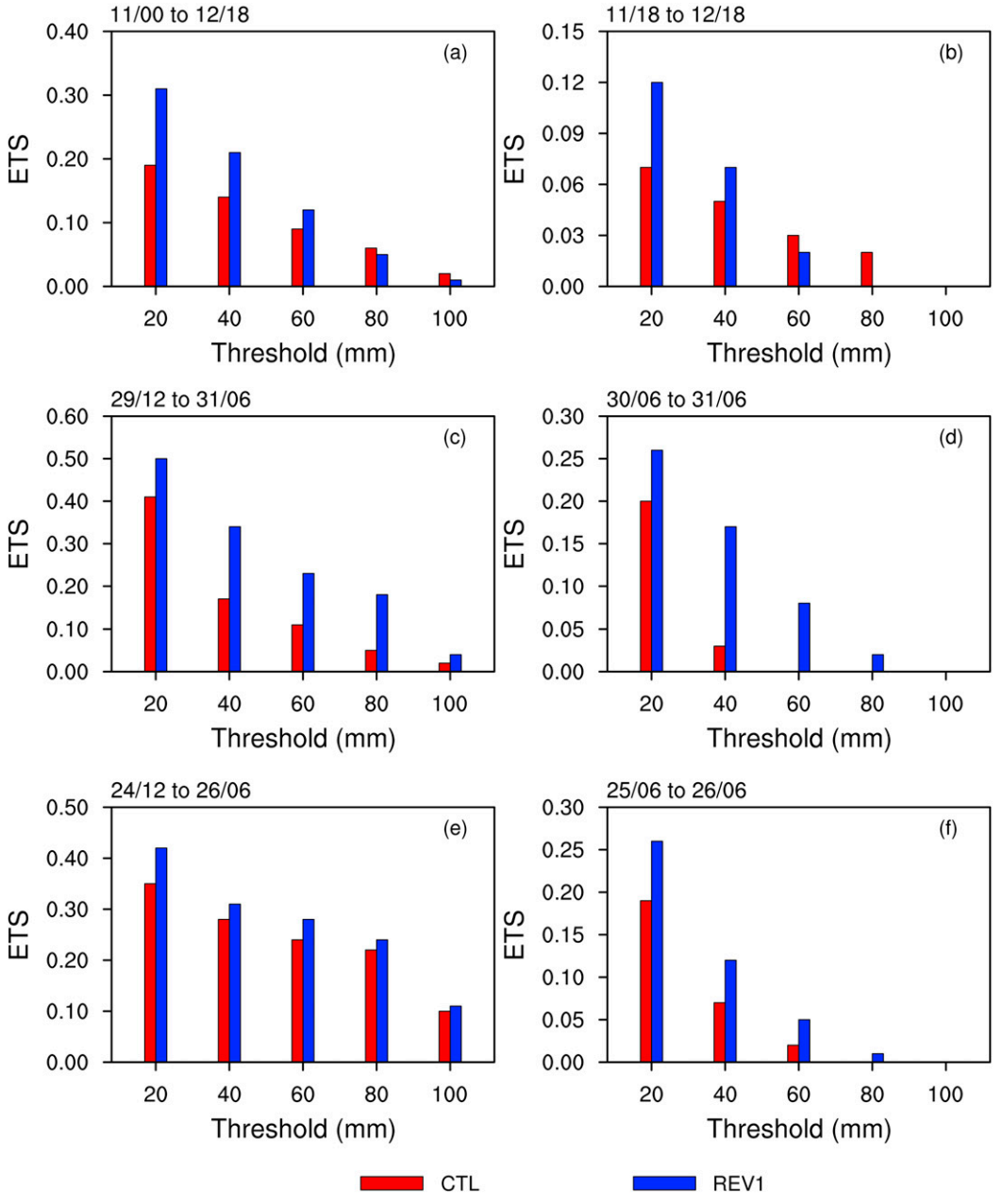

FIG. 8. Comparison of ETS for (a),(c),(e) 42-h (36–78-h forecasts) and (b),(d),(f) 24-h accumulated precipitation (54–78-h forecasts) for (a),(b) Hurricane Dennis, (c),(d) Hurricane Katrina, and (e),(f) Hurricane Rita in different experiments against CCPA precipitation analysis with thresholds of 20, 40, 60, 80, and 100 mm.

with the land surface, the environmental θ_e around the warm core in REV1 is weaker than that in CTL. In other words, a more obvious cold and dry environment around the warm core resulting from the modified K_m contributes to more efficient hurricane decay. This agrees well with previous studies that the incorporation of dry and cold air from the environment by the hurricane's secondary circulation along the warm core is an important reason for hurricane decay (Powell 1990; Kimball 2006). As a result, the warm core and the inflow/outflow vanish earlier in REV1 (Figs. 11g–j) than that in CTL (Figs. 11b–e). The evolution of azimuthally averaged vertical velocity in Fig. 12 is similar to that in Fig. 11. During and after landfall, the vertical motion in REV1 is always weaker than that in CTL. Upon the gradual decay of the vortex, the vertical motion dissipates in REV1 (Fig. 12j), while it is still active in CTL (Fig. 12e) at the end of the simulation. Another noticeable characteristic

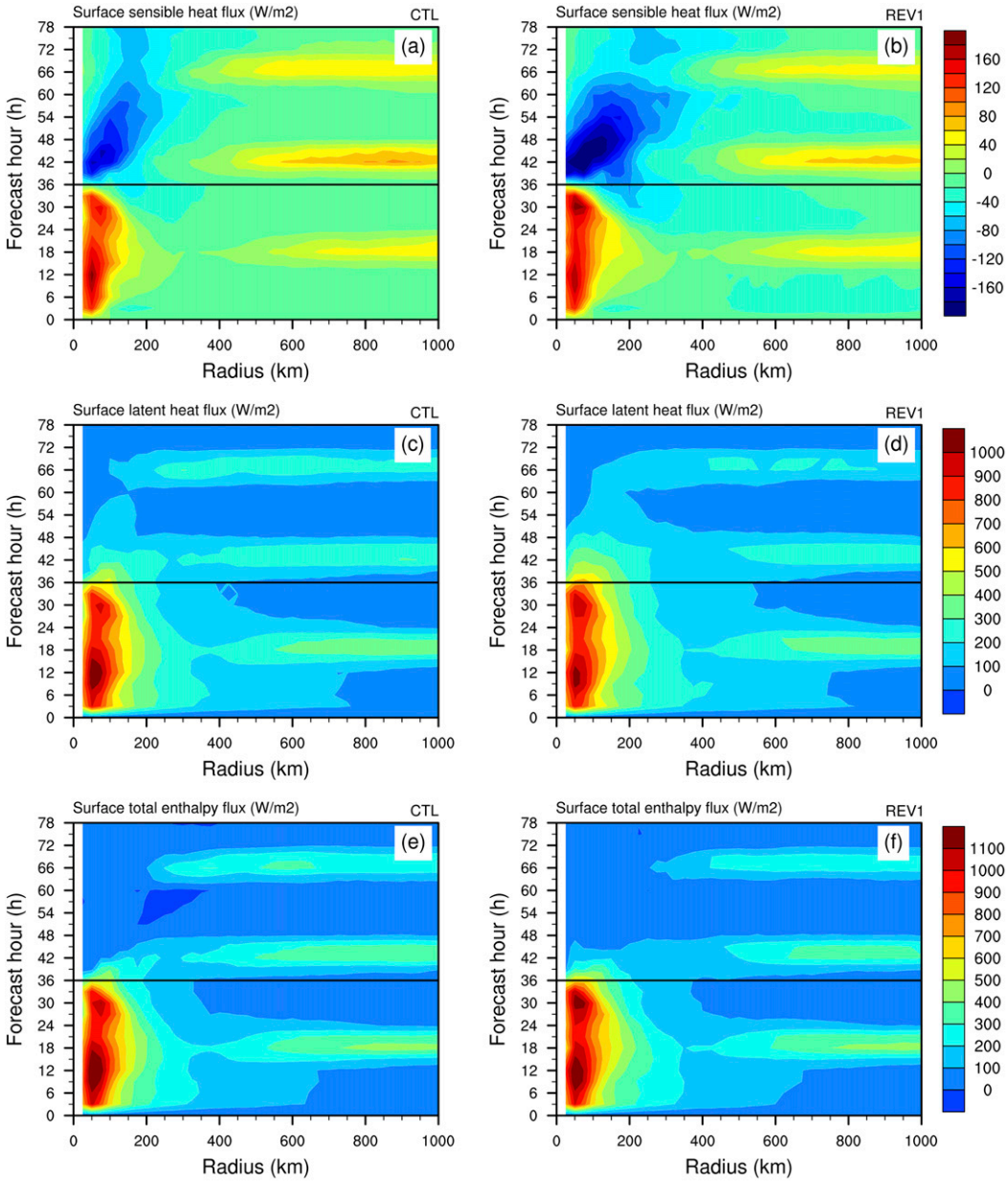

FIG. 9. Azimuthally averaged surface (a),(b) sensible heat fluxes (W m^{-2}); (c),(d) latent heat fluxes (W m^{-2}); and (e),(f) total enthalpy fluxes (W m^{-2}) during the evolution of Hurricane Rita from ocean to land throughout the period of numerical simulations (from 0000 UTC 23 Sep to 0600 UTC 26 Sep 2005). The *x* axis represents the radius from the storm center, and the *y* axis represents the forecast hour from the initial time. The solid black line represents the approximate landfall time.

in Figs. 11 and 12 is that REV1 produces a lower PBLH than CTL while the hurricane interacts with the land surface.

Figure 13 shows the azimuthally averaged θ_e within a radius of 300 km from the storm center at 900 hPa θ_{e_900} and the θ_e difference between 900 hPa and surface (θ_{e_900} minus θ_{e_sfc}). Compared to CTL, both θ_{e_900} and $\theta_{e\_900} - \theta_{e\_sfc}$ decrease more rapidly after the hurricane moves from the ocean to land in REV1, indicating stronger vertical mixing that results in the rapid decrease of θ_e within the hurricane boundary layer.

Figure 14 compares the azimuthally averaged temperature anomalies and tangential wind speeds between 1000- and 100-hPa pressure levels before, during, and after hurricane landfall for CTL (left) and REV1 (right). Over the ocean at the 18-h forecast (Figs. 14a,f), REV1

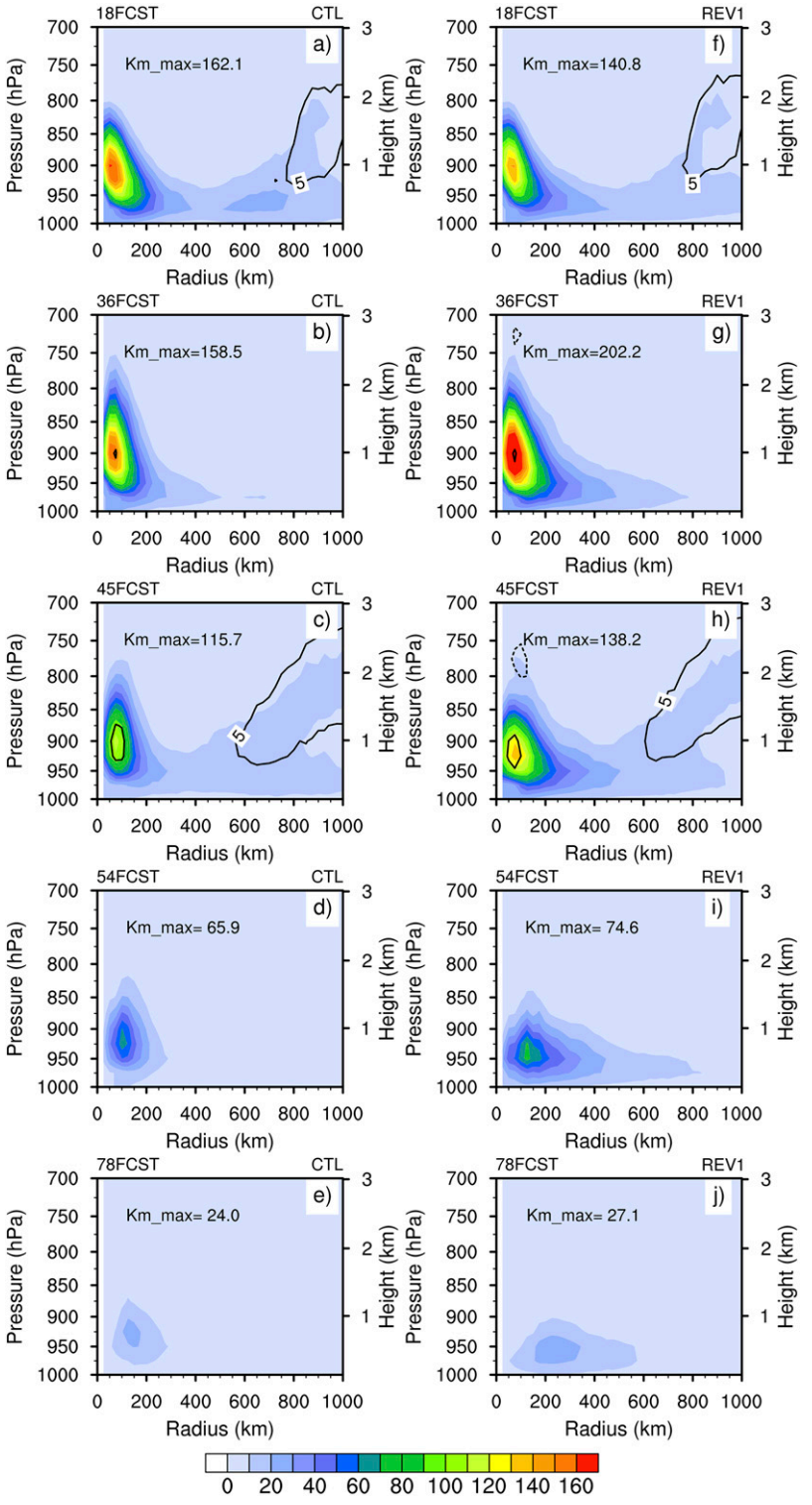

FIG. 10. Azimuthally averaged vertical eddy diffusivity ($m^2 s^{-1}$) for momentum K_m (shaded) and the difference between thermal and momentum (K_h minus K_m; contour interval is $5 m^2 s^{-1}$; positive values denoted as a solid line, negative values denoted as a dashed line) during the evolution of Hurricane Rita from ocean to land at (a),(f) 18-; (b),(g) 36-; (c),(h) 45-; (d),(i) 54-; and (e),(j) 78-h forecasts. (a)–(e) CTL, and (f)–(j) REV1. The initial time is 0000 UTC 23 Sep 2005.

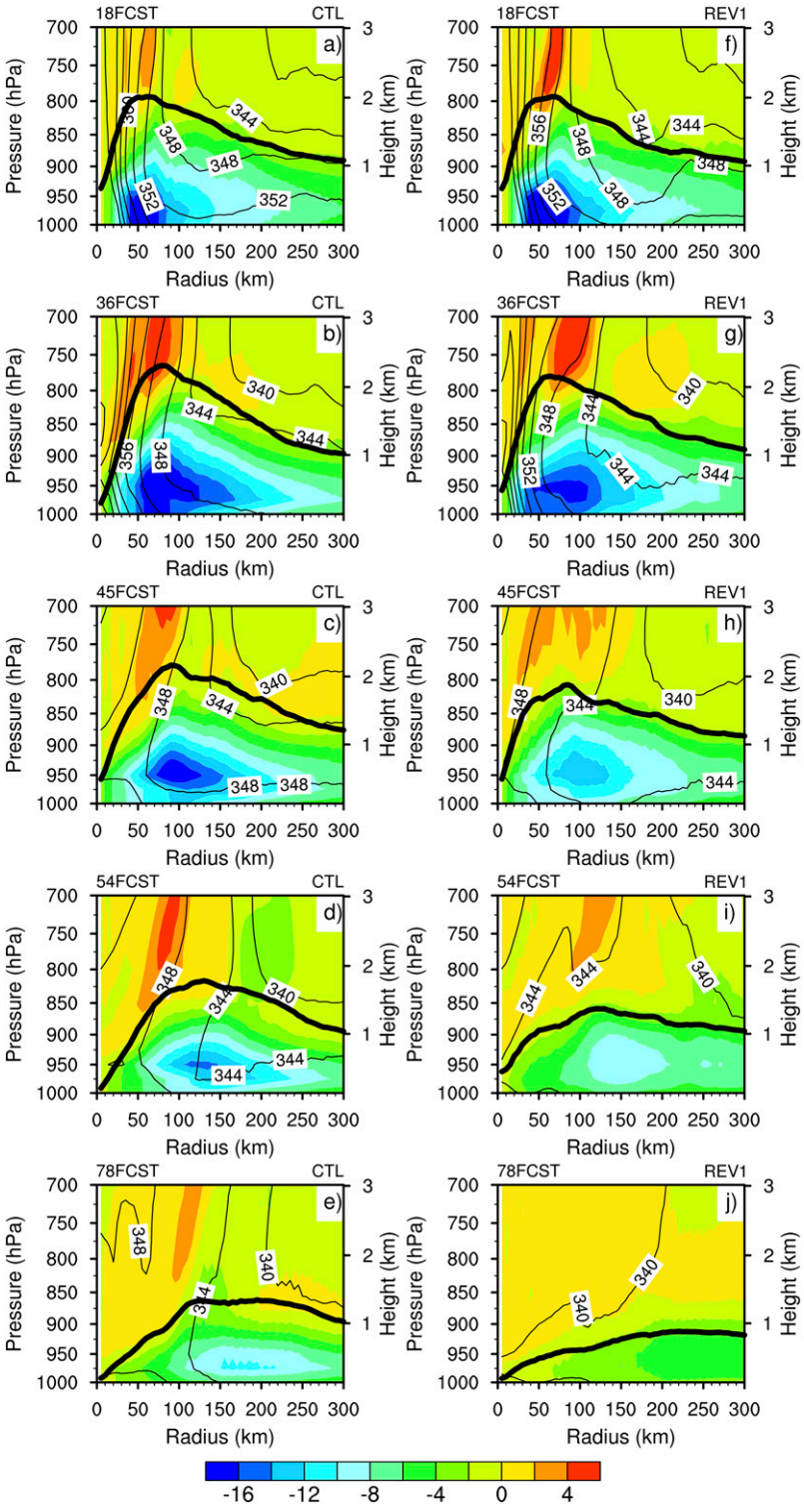

FIG. 11. Azimuthally averaged θ_e (thin contours; K) and radial wind (shaded; m s^{-1}) below 700 hPa at (a),(f) 18; (b),(g) 36; (c),(h) 45; (d),(i) 54; and (e),(j) 78 h for Hurricane Rita from 00 UTC 23 Sep 2005. (a)–(e) CTL and (f)–(j) REV1. The *x* axis represents the radius from the storm center, and the bold solid line represents PBLH (m).

produces slightly stronger hurricane intensity in terms of the warm core and tangential wind speed, compared with CTL. During and after landfall, the hurricane weakens with obvious decreases in both the warm-core temperature and the tangential wind (Figs. 14b–e and 14g–j) that are greater in REV1 than in CTL. Since the cooling of the upper and middle levels of the storm is ultimately responsible for the hydrostatic increase in the central pressure necessary to reduce the pressure gradient and weaken the hurricane after landfall (Shapiro and Willoughby 1982; Powell 1987), therefore, the simulated hurricane in REV1 decays more efficiently than that in CTL. As a consequence, the hurricane intensity (surface wind, surface pressure, and its gradient) is well portrayed in REV1 (with modified K_m) but overestimated in CTL (as shown in Figs. 3 and 6).

The evolution of divergence and vorticity fields also responded accordingly. Figure 15 illustrates the time-averaged vertical profile of mean absolute vorticity (bottom) and divergence (top) within a radius of 300 km from the storm center over ocean (ocean) and land (right). Compared to CTL, the simulated storm by REV1 is slightly stronger in terms of lower-level convergence and upper-level divergence over the ocean (Fig. 15a). When the hurricane moves over land, however, the convergence/divergence weaken more effectively in REV1 (Fig. 15b) when compared to CTL. The vorticity fields in Figs. 15c and 15d also indicate that REV1 tends to produce a storm with a slightly stronger spiral feature over the ocean but attenuates more rapidly in case of the hurricane over land when compared to CTL. According to Cram et al. (2007), strong spiral vortices (as simulated by CTL) tend to result in the insufficient decay of a hurricane during and after its landfall.

Figure 16 compares the observation-based hurricane surface wind analysis from NOAA HRD (Powell and Houston 1996) to the simulated surface wind at the 36-h forecast, valid at 1200 UTC 24 Sep 2005. Results show that the peak surface wind speed of observation is located over the ocean, while it is located over the land in both CTL and REV1. However, compared to the CTL, REV1 produces more reasonable surface winds that are closer to the HRD analysis in terms of the magnitude and distribution of wind speeds. This is especially true in the east and southeast quadrants (white box in Fig. 16), where surface winds are over 48 m s^{-1} in CTL in a larger area than that in REV1. Specifically, the observed maximum wind speeds are about 49 m s^{-1}, and the simulated maximum wind speeds are 54 m s^{-1} in CTL and 50 m s^{-1} in REV1.

Many previous studies have emphasized the importance of convective rainbands along the warm core (Powell 1990; Houze et al. 2006), which act as a barrier and delineate the transition between the warm-core region and the environment surrounding the storm (Willoughby et al. 1984). In addition, the low-level (i.e., 850 hPa) distribution of θ_e is also an important indicator of the interactions between hurricane vortices and environmental air (Powell 1987). Figures 17 and 18 illustrate the horizontal distribution of θ_e and radar reflectivity, respectively. When the hurricane is over the ocean (Figs. 17a,f and 18a,f), both θ_e and radar reflectivity are well organized in the hurricane inner-core region. The hurricane eye is clear, and outer rainbands are concentric to the eyewall in both CTL and REV1. Then, during hurricane landfall (Figs. 17b,g and 18b,g), the rainbands begin to break up, and the spiral structures start to deform. Compared with CTL, θ_e along the warm core is much weaker in REV1 at northwest and northeast quadrants, which is important to the weakening of the warm core. The simulated reflectivity shows that the rainbands in REV1 are similar to CTL at this time, with broken structures the northeast of the hurricane center. After landfall, θ_e and reflectivity continue to weaken. Figures 17c–e and 17h–j show that, influenced by the lower θ_e, the warm core decays more obviously in REV1 than in CTL. Figures 18c–e and 18h–j also depict that the simulated radar reflectivity in REV1 is weaker and has a looser and less organized structure than that in CTL during the evolution over land, especially after the 54-h forecast. In particular, the spiral storm structures disappear in REV1, while they remain in CTL by the end of the simulation (Figs. 17e,j and 18e,j), implying that the dissipation of convective rainbands is effective in the simulation with the modified K_m but ineffective in the simulation with the original parameterization. Furthermore, the weaker convergence in the modified K_m (Fig. 15) also suggests that the convergence associated with the convective rainbands is weaker than that in the original scheme, therefore, inhibiting the development of convective activity.

The evolution of rainband structures agrees well with the simulated precipitation. For example, Figs. 18d–e and 18i–j (54–78-h forecasts) indicate that the simulated reflectivity is stronger and has a more organized structure in CTL but is weaker and less organized in REV1. In addition, the simulated reflectivity extends to the northeast of the hurricane center in REV1 and is missed in CTL. These characteristics are in accord with the simulated precipitation as shown and discussed in Figs. 7g–i. Therefore, the overestimated rainfall amount and the missed part of the rainfall in the northeast in the simulation with the original scheme are ably remedied in the simulation with modified K_m (Figs. 7g–i). Similar

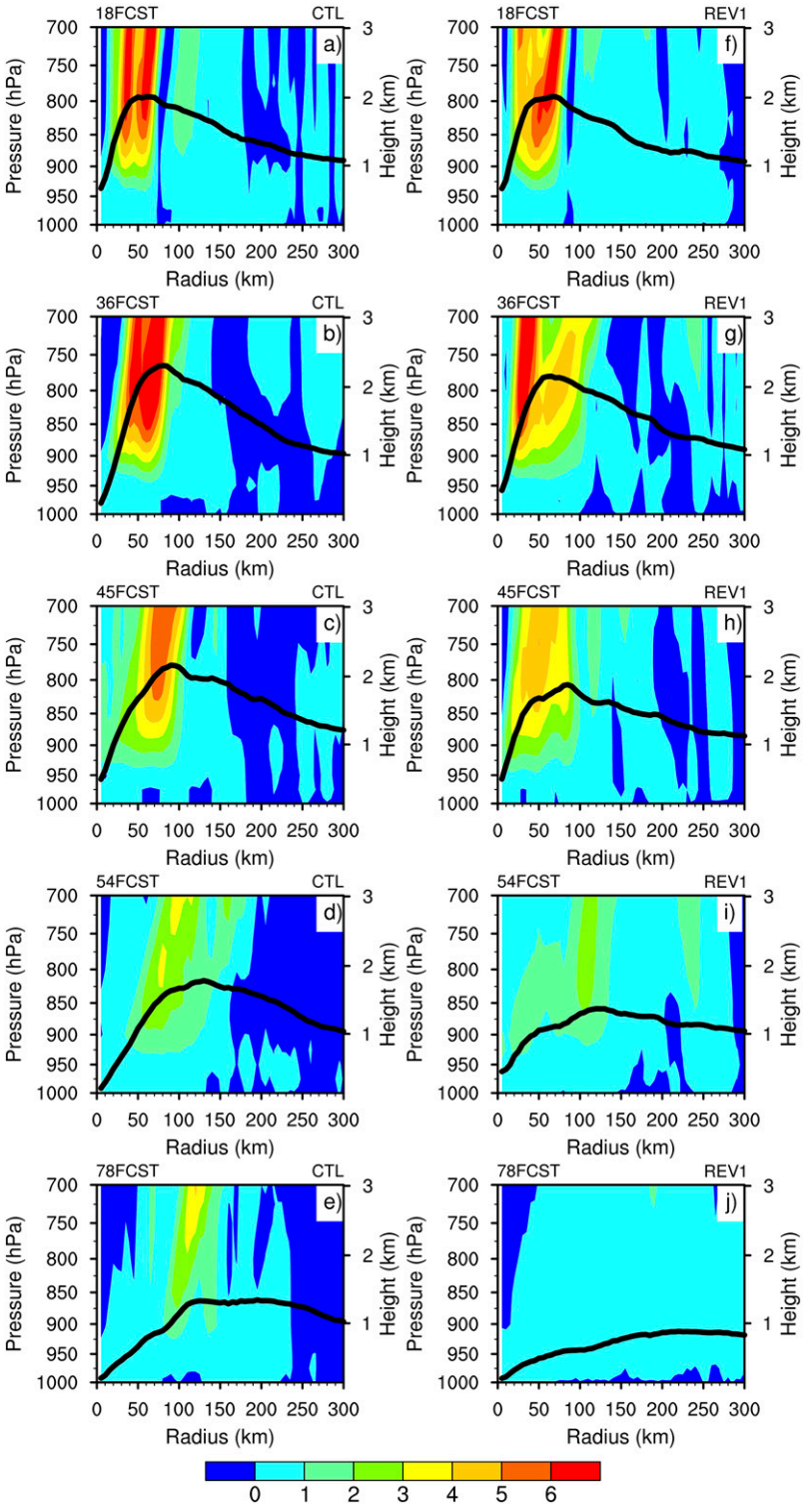

FIG. 12. As in Fig. 11, but for vertical velocity ($\times 10$; m s^{-1}) below 700 hPa.

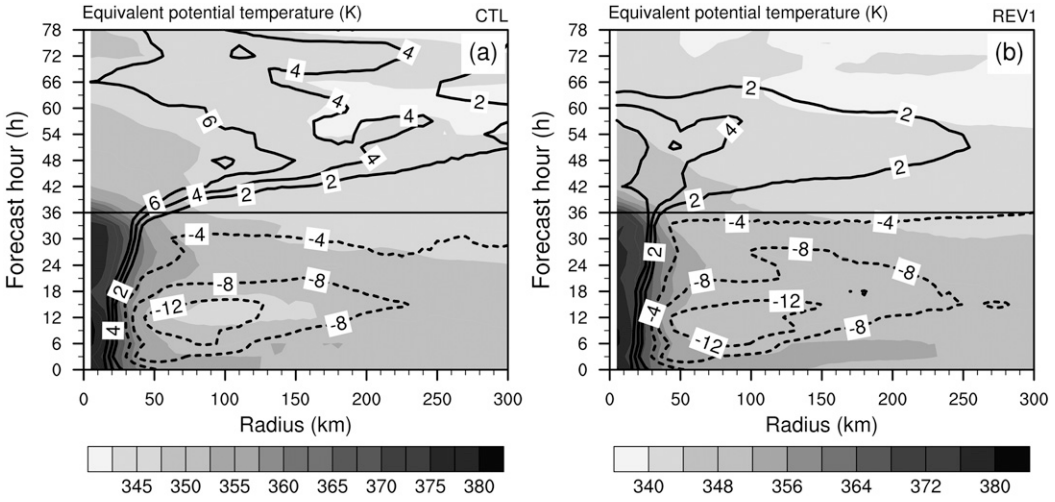

FIG. 13. Azimuthally averaged θ_e at 900 hPa (shaded; K) and the difference of θ_e between 900 hPa and surface (θ_{e_900} minus θ_{e_sfc}; contours, dashed for negative; K). The x axis represents the radius from the storm center, and the y axis represents the forecast hour from the initial time. The horizontal solid black line represents the approximate landfall time.

results are also found with numerical simulations for Hurricanes Katrina and Dennis (not shown).

5. Discussion

Previous studies have revealed that the significant reduction of surface heat and moisture fluxes are mainly responsible for a hurricane's decay during its landfall (Miller 1964; Rosenthal 1971; Powell 1982, 1987; Kimball 2006). A recent study by Davis et al. (2008) pointed out that insufficient enthalpy (heat and moisture) exchange with the surface is an unavoidable recurring error which occurs when predicting landfalling hurricanes. Results presented in sections 4 and 5 illustrated that the modified K_m improves the simulation of landfalling hurricanes, as it makes vertical mixing in the PBL more efficient.

To further interpret the effects of the modified K_m on vertical mixing in the PBL, Fig. 19 shows the azimuthally averaged u_*, ϕ_m, w_{*b}, and w_s during the hurricane evolution from ocean to land based on Eqs. (3) and (6). Over the core region of the storm, the evolution of u_* in the original K_m (Fig. 19a) is similar to the modified K_m (Fig. 19b), as both present a uniform feature over the ocean and a rapid increase during and shortly after hurricane landfall, as well as its gradual decrease when the hurricane moves farther inland. Also, the decrease of u_* in the modified K_m is more obvious than in the original K_m during the 48–78-h forecast. This is mainly because of the more rapid decay of hurricane surface wind.

Meanwhile, over the core region of the storm, ϕ_m values in both experiments with original (Fig. 19c) and modified K_m schemes (very similar to Fig. 19c, not shown) are about 0.6–1.0 over the ocean and increase gradually when the hurricane interacts with the land surface (greater than 1.0), suggesting that the lower level of the hurricane is slightly unstable and close to neutral over the ocean but becomes stable over land, according to the flux–profile relationship (e.g., Businger et al. 1971). This could also be inferred from Fig. 9 that surface sensible heat flux is positive over ocean but negative over land. The evolution of w_{*b} (Fig. 19d) in the modified K_m, however, is significantly larger over the ocean but decreases rapidly when the hurricane moves inland, suggesting that w_{*b} is only important when the hurricane is over the ocean but is negligible when it interacts with the land surface.

Therefore, during and after hurricane landfall, w_s in the original K_m scheme tends to decrease because of the large ϕ_m as shown in Fig. 19e, according to Eq. (3). However, in the modified scheme, w_s approaches u_* as shown in Fig. 19f, according to Eq. (6). As a result, vertical mixing in the PBL with the modified K_m scheme (Figs. 10g–j) is more efficient than that with the original scheme (Figs. 10b–e).

On the other hand, when a hurricane evolves over the ocean, vertical mixing in the PBL (Figs. 10a,f) in the modified K_m is very similar to the original K_m with a maximum reduction at about 22 $m^2 s^{-1}$ (~13%), which is in agreement with the results of Figs. 19e and 19f: namely, w_s in REV1 is slightly smaller than that in CTL. This suggests that Eq. (6), which includes the vertical transport of buoyancy fluxes ($kw_{*b}^3 z/h$) term, does not fundamentally affect vertical mixing in the PBL when compared to

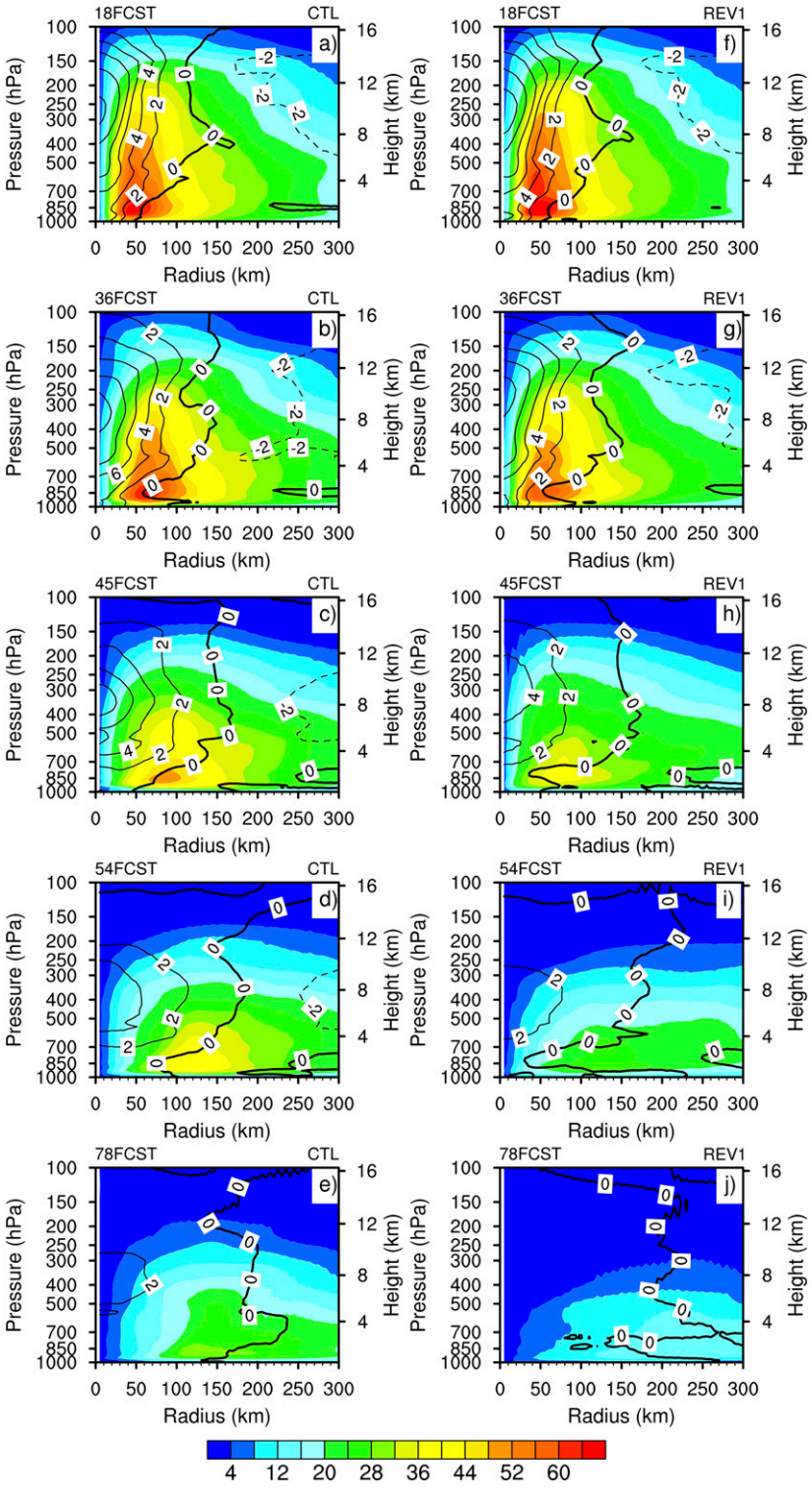

FIG. 14. Azimuthally averaged temperature anomaly (contours; K) and tangential wind speed (shading; m s^{-1}) from 1000 to 100 hPa during the evolution of hurricanes from ocean to land at (a),(f) 18-; (b),(g) 36-; (c),(h) 45-; (d),(i) 54-; and (e),(j) 78-h forecasts for Hurricane Rita starting from 0000 UTC 23 Sep 2005. (a)–(e) CTL and (f)–(j) REV1. The *x* axis represents the radius from the storm center.

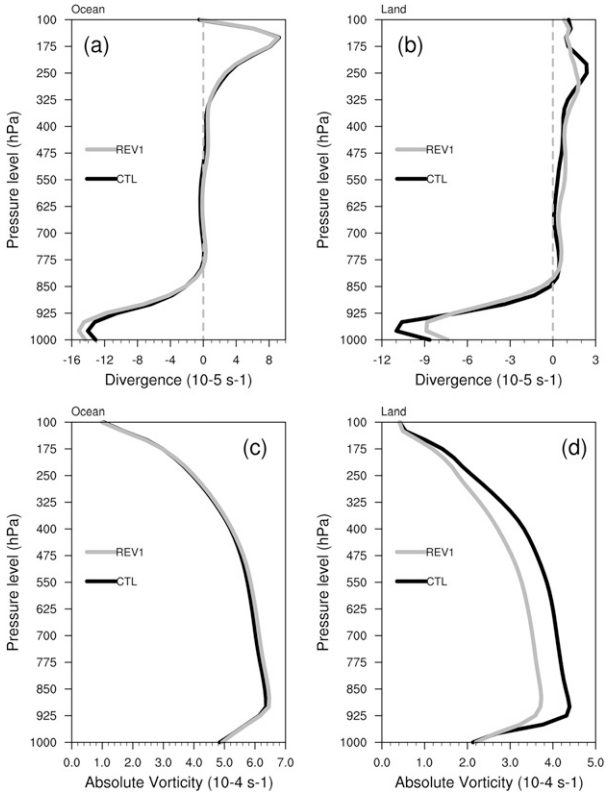

FIG. 15. Time-averaged vertical profile of (a),(b) mean divergence ($\times 10^5\ s^{-1}$) and (c),(d) absolute vorticity ($\times 10^4\ s^{-1}$) with a radius of 300 km from storm center over (a),(c) ocean and (b),(d) land.

Eq. (3). The finding here agrees with previous findings by Nicholls (1985) and Zhang et al. (2009) that the turbulence production by buoyancy is less important in the tropical cyclone. In addition, recent studies by Zhang et al. (2015) and Gopalakrishnan et al. (2013) used an α method to modulate the vertical eddy diffusivity. They found this method could cause an unphysical inconsistency between the boundary layer and the surface layer schemes. The modification in this study would not fix this problem because $\alpha \neq 1$ in this study. However, the patterns of the simulated vertical eddy diffusivity, as shown in Figs. 10a and 10f, agree well with their results. The maximum vertical eddy diffusivity is located around the storm center. Moreover, the magnitude of simulated K_m in both CTL and REV1 over the ocean is also consistent with the observational results from Zhang et al. (2015).

As stated in section 3, the modification of mixed-layer velocity scale w_s in the REV1 experiment [e.g., Eq. (6)] is the same as in the YSU scheme but for both stable and unstable conditions. To further examine the sensitivity of the simulation of a landfall hurricane to the parameterization of vertical eddy diffusivity in PBL, an additional set of experiments (REV2; see Table 1) that is the same as the YSU scheme (Hong and Pan 1996), with w_s as defined in Eqs. (3) and (6) under stable and unstable stratifications, respectively, is conducted for Hurricane Rita. Results (Fig. 20) indicate that the simulated hurricanes are basically the same as those obtained from the original HWRF regarding track and intensity, suggesting the important role of the vertical eddy diffusivity in the predicting landfalling hurricanes.

Moreover, results from this study show that the strong vertical mixing in the PBL tends to result in a shallow PBLH (determined by critical Richardson number method; Troen and Mahrt 1986) during and after the hurricane landfall (over land; Figs. 11, 12), which is opposite to the relationship over the ocean (Kepert 2012).

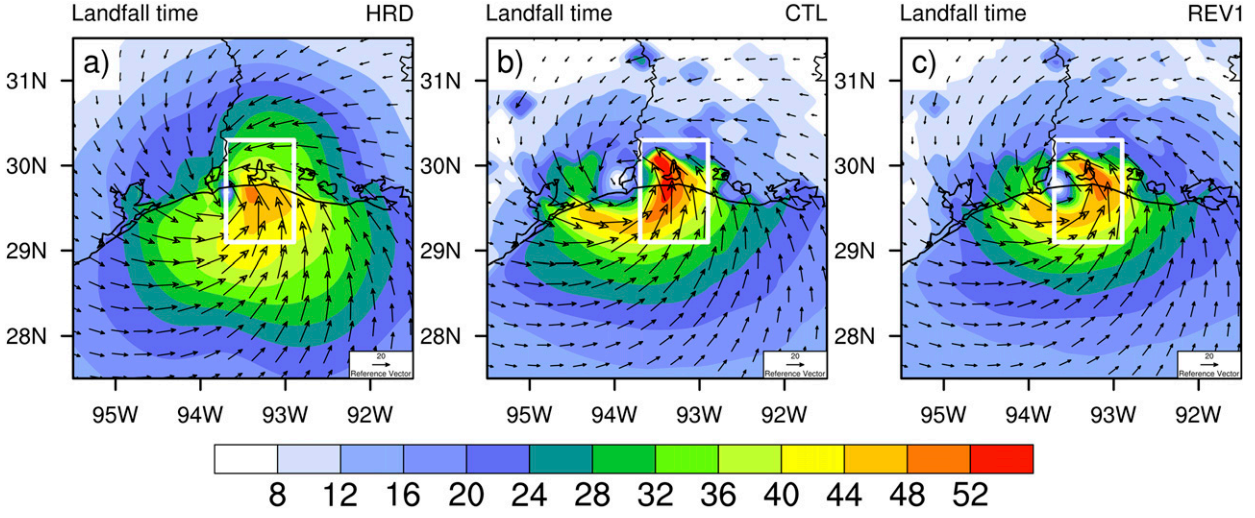

FIG. 16. Surface wind ($m\ s^{-1}$) at landfall time (36-h forecast, valid at 1200 UTC 24 Sep 2005) for Hurricane Rita. (a) HRD analysis (courtesy of http://www.hwind.co/legacy_data/), (b) CTL, and (c) REV1.

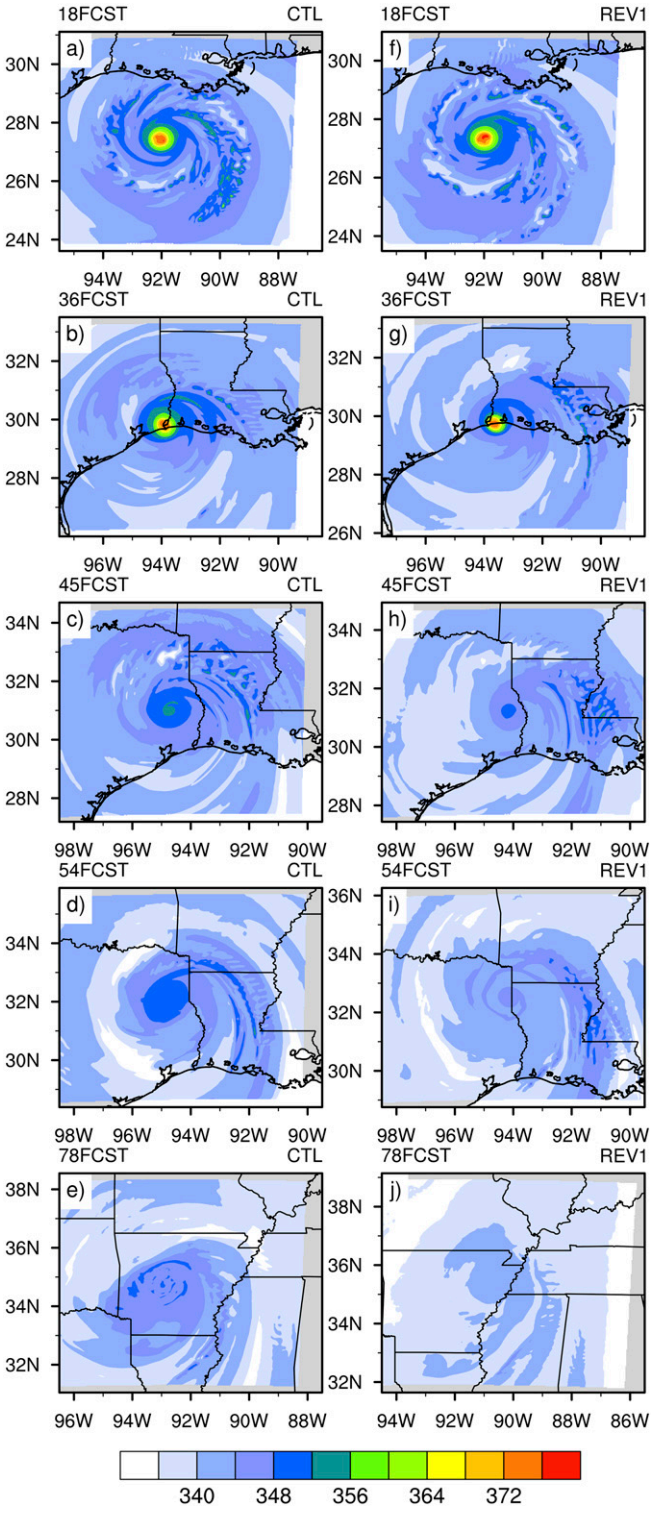

FIG. 17. Horizontal θ_e (K) at 850 hPa for Hurricane Rita during its evolution from ocean to land at (a),(f) 18-; (b),(g) 36-; (c),(h) 45-; (d),(i) 54-; and (e),(j) 78-h forecasts from 0000 UTC 23 Sep 2005. (a)–(e) CTL and (f)–(j) REV1.

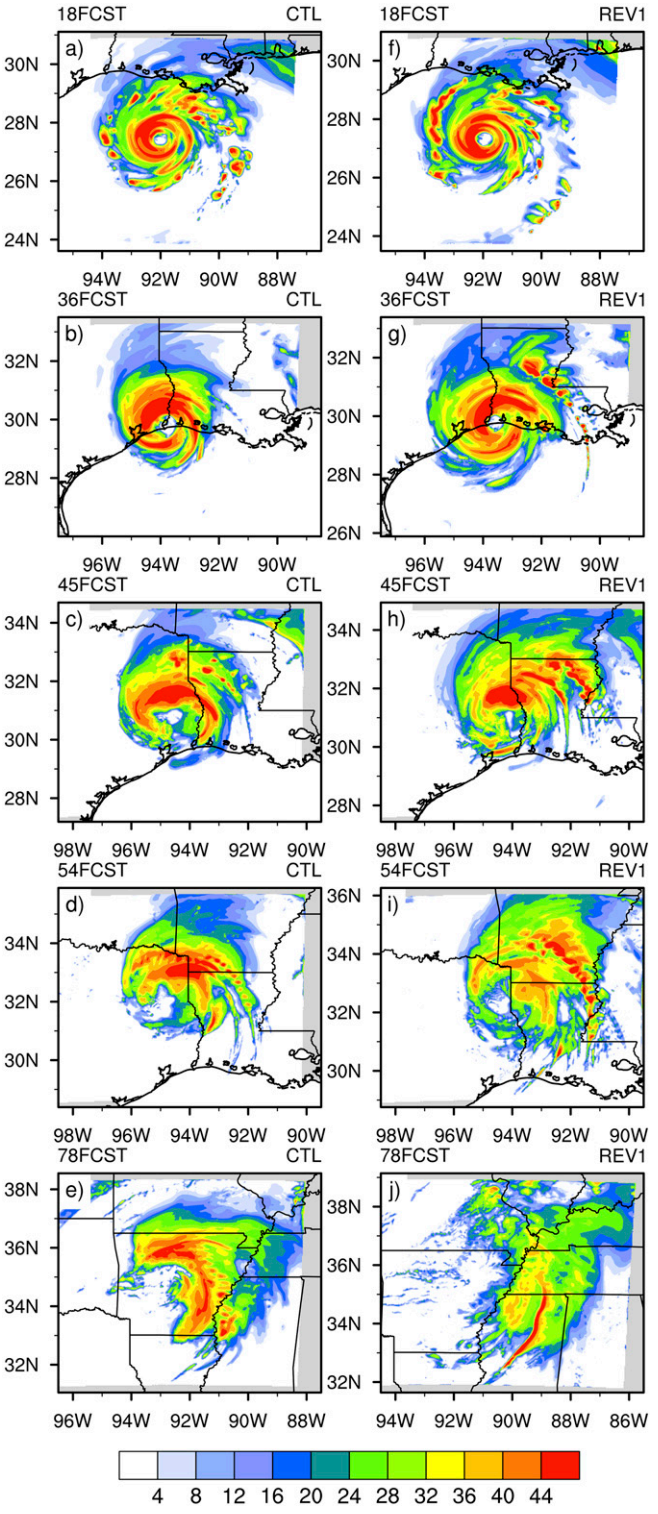

FIG. 18. As in Fig. 17, but for composite radar reflectivity (dBZ).

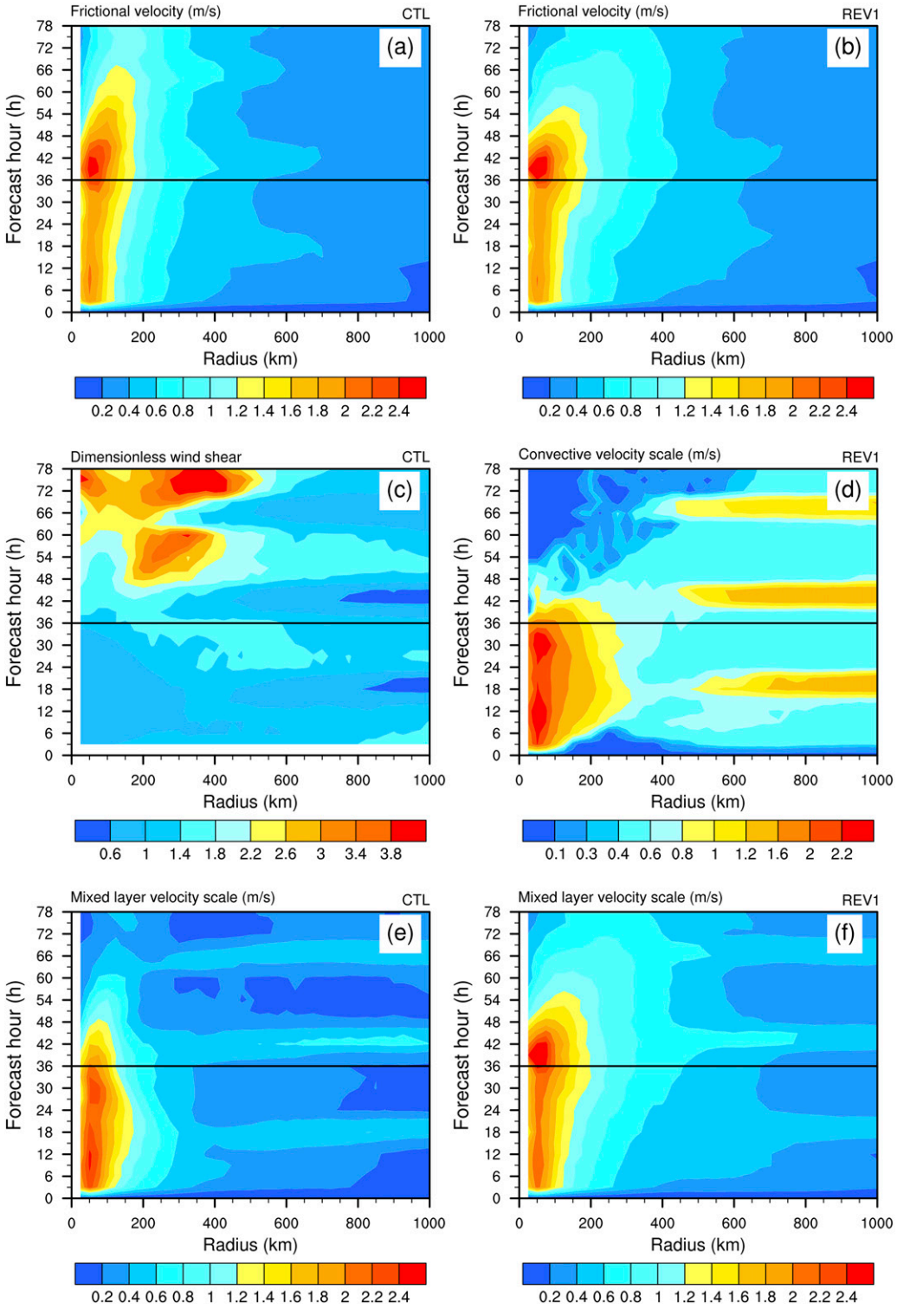

FIG. 19. As in Fig. 9, but for (a),(b) surface frictional velocity u_* ($\mathrm{m\,s^{-1}}$) from (a) CTL and (b) REV1; (c) dimensionless wind shear at the top of surface layer ϕ_m from CTL; (d) convective velocity scale w_{*b} ($\mathrm{m\,s^{-1}}$) from REV1; and (e),(f) mixed-layer velocity scale w_s ($\mathrm{m\,s^{-1}}$) from (e) CTL and (f) REV1.

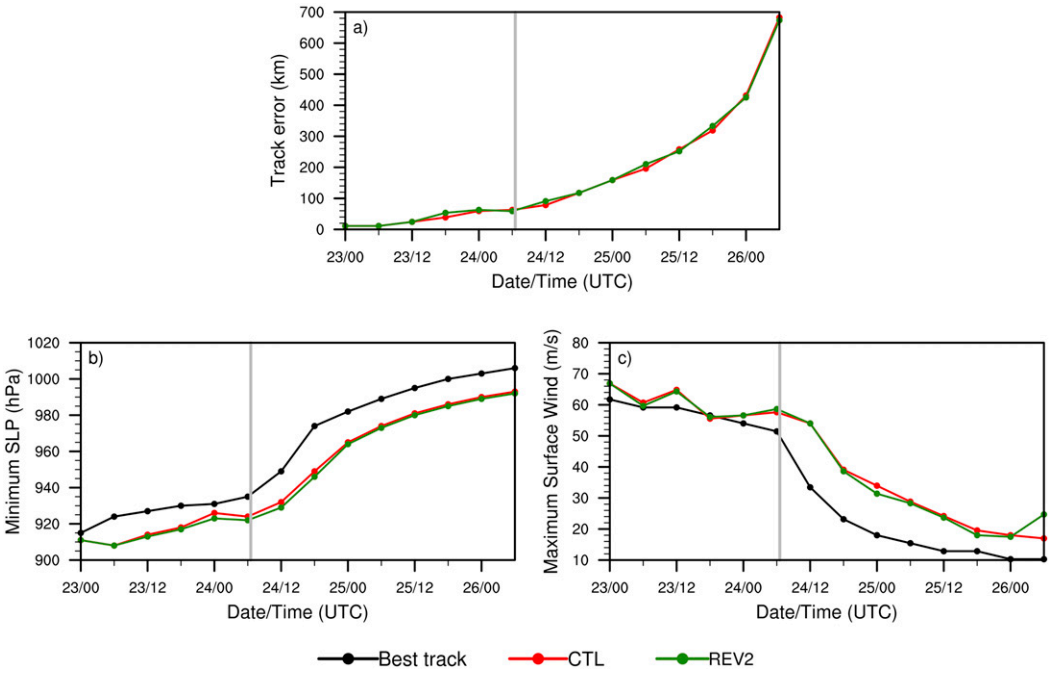

FIG. 20. As in Fig. 3, but for the comparison between CTL and REV2 experiments against NHC best-track data.

To explain the reason behind these differences, the definition of PBLH has to be revisited. In theory, Kepert (2012) indicates that the maximum and mean K_m could be derived as follows:

$$K_{\max} = ku_*h\frac{p^p}{(p+1)^{p+1}} \quad \text{and} \tag{8}$$

$$\overline{K} = \frac{ku_*h}{(p+1)(p+2)}. \tag{9}$$

It is apparent that both $K_{\max}$ and $\overline{K}$ are proportional to h, or vice versa. Specifically, in Kepert's study, the hurricane boundary layer is assumed to be near neutral, which could be reasonable for a hurricane over the ocean because ϕ_m is near 1.0 (Fig. 19c) and u_* tends to be uniform with time (Figs. 19a,b). During and after hurricane landfall, however, both ϕ_m and u_* change significantly (Figs. 19a–c). The influence of u_* and ϕ_m terms on K_m becomes significant (Fig. 19) over land; thus, ϕ_m should also be considered in Eqs. (8) and (9). Taking Eq. (3), for instance, Eqs. (8) and (9) become

$$K_{\max} = k\frac{u_*}{\phi_m}h\frac{p^p}{(p+1)^{p+1}} \quad \text{and} \tag{10}$$

$$\overline{K} = \frac{k(u_*/\phi_m)h}{(p+1)(p+2)}. \tag{11}$$

Therefore, both $K_{\max}$ and $\overline{K}$ are not linearly proportional to h. This explains the reason why the PBLH is not proportional to vertical mixing in the PBL during hurricanes evolution over land, or vice versa.

To further confirm the rationality of PBLH evolution in CTL and REV1 (Figs. 11, 12), Fig. 21 compares the bulk Richardson number ($R_{ib} = g\Delta\overline{\theta_v}\Delta z/\{\overline{\theta_v}[(\Delta\overline{U})^2 + (\Delta\overline{V})^2]\}$; Stull 1988), which is an important scale to represent atmospheric stability. Results show that R_{ib} increased gradually during hurricane evolution from ocean to land, especially in REV1. As a consequence, the efficient increase of R_{ib} in the PBL with the modified K_m would produce a shallow PBLH according to the definition of PBLH in HWRF, as mentioned in section 3.

6. Concluding remarks

Hurricanes undergo a weakening process during their evolution that depends on the surface and atmospheric conditions over land. Based on studies of the landfalls of three hurricanes (Dennis, Rita, and Katrina) in 2005, this paper evaluates the effects of vertical eddy diffusivity parameterizations for momentum K_m on the simulated tracks, intensities, and structures of the hurricanes and their associated QPFs. It is found that the vertical eddy diffusivity in the original HWRF tends to produce stronger hurricanes than the observations with much lower surface pressures, stronger surface winds, and larger track errors during their evolution over land. With the modified K_m based on the change of the mixed-layer velocity scale for both stable and unstable

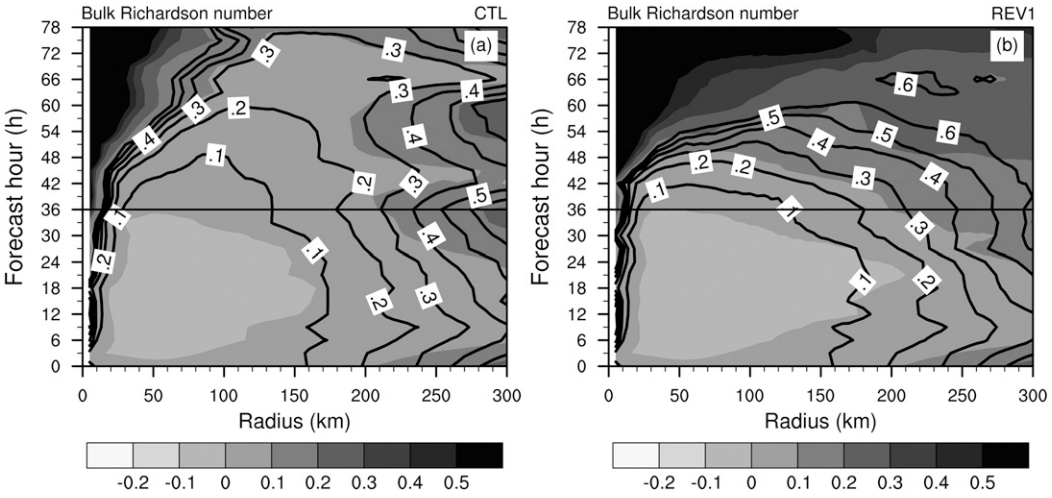

FIG. 21. As in Fig. 9, but for R_{ib} at 900 (shaded) and 850 hPa (contours) in (a) CTL and (b) REV1.

conditions, vertical mixing in the hurricane boundary layer becomes efficient over land, leading to more realistic and efficient hurricane decay over land. As a result, the simulated hurricane track, intensity, and QPFs are improved.

Further diagnoses show that, because of the modification of K_m, both the kinematic and thermodynamic structures of the hurricane vortices are well portrayed. Specifically, the impacts of vertical eddy diffusivity parameters are mainly on hurricane inner-core structures. Overall, with the efficient vertical mixing in the hurricane boundary layer, the simulated storms are weaker and have a shallower PBL, weaker inflow/outflow, weaker warm core, and weaker spiral wind structure, as well as weaker, looser, and less organized convective rainbands.

The framework proposed in this study is expected to be useful for understanding the role of vertical mixing in the PBL parameterization on landfalling hurricanes and their evolution, especially over land. Results in this study should have implications for future improvements in PBL schemes. However, it should be noted that the results of this study should not be used as a commentary on how to improve the parameterization of the vertical eddy diffusivity in HWRF since the sensitivity experiments in this study focused on only three hurricanes that made landfall in the Gulf of Mexico and underwent decay processes. Future work should focus on more landfall cases with a larger sample size, as well as on hurricane reintensification over land. In addition, the mismatches between the surface-layer and boundary layer schemes, as well as the associated impacts on hurricane evolution, also deserve further discussion when turbulence observations within the hurricane boundary layer are available, especially during and after hurricane landfall. In addition, land-surface processes (soil state, etc.) and surface-layer parameterization should also be considered in future work in order to fully address the interaction between hurricane vortices and land processes.

Acknowledgments. This study is supported by National Science Foundation Award AGS-1243027 (Pu and Zhang), Office of Naval Research Award N000141612491 (Pu), and NOAA Grant NA14NWS4680025 (Pu). High-performance computing support from Yellowstone (ark:/85065/d7wd3xhc), provided by NCAR's Computational and Information Systems Laboratory (CISL) and the Center for High-Performance Computing (CHPC) at the University of Utah, are greatly appreciated. Comments from Prof. Chun-Chieh Wu and three anonymous reviewers were very helpful for improving the early version of the manuscript.

REFERENCES

Bao, J. W., S. A. Michelson, and J. M. Wilczak, 2002: Sensitivity of numerical simulations to parameterizations of roughness for surface heat fluxes at high winds over the sea. *Mon. Wea. Rev.*, **130**, 1926–1932, doi:10.1175/1520-0493(2002)130<1926:SONSTP>2.0.CO;2.

Beven, J., 2005: Tropical cyclone report: Hurricane Dennis, 4–13 July 2005. NOAA/National Hurricane Center Rep., 25 pp. [Available online at http://www.nhc.noaa.gov/data/tcr/AL042005_Dennis.pdf.]

Bluestein, H. B., and D. S. Hazen, 1989: Doppler-radar analysis of a tropical cyclone over land: Hurricane Alicia (1983) in Oklahoma. *Mon. Wea. Rev.*, **117**, 2594–2611, doi:10.1175/1520-0493(1989)117<2594:DRAOAT>2.0.CO;2.

Braun, S. A., and W. K. Tao, 2000: Sensitivity of high-resolution simulations of Hurricane Bob (1991) to planetary boundary layer parameterizations. *Mon. Wea. Rev.*, **128**, 3941–3961, doi:10.1175/1520-0493(2000)129<3941:SOHRSO>2.0.CO;2.

Brettschneider, B., 2008: Climatological hurricane landfall probability for the United States. *J. Appl. Meteor. Climatol.*, **47**, 704–716, doi:10.1175/2007JAMC1711.1.

Businger, J. A., J. C. Wyngaard, Y. Izumi, and E. F. Bradley, 1971: Flux-profile relationships in the atmospheric surface layer. *J. Atmos. Sci.*, **28**, 181–189, doi:10.1175/1520-0469(1971)028<0181:FPRITA>2.0.CO;2.

Chen, S. S., W. Zhao, M. A. Donelan, J. F. Price, and E. J. Walsh, 2007: The CBLAST-Hurricane Program and the next-generation fully coupled atmosphere–wave–ocean models for hurricane research and prediction. *Bull. Amer. Meteor. Soc.*, **88**, 311–317, doi:10.1175/BAMS-88-3-311.

Cione, J., E. A. Kalina, J. A. Zhang, and E. W. Uhlhorn, 2013: Observations of air–sea interaction and intensity change in hurricanes. *Mon. Wea. Rev.*, **141**, 2368–2382, doi:10.1175/MWR-D-12-00070.1.

Cram, T. A., J. Persing, M. T. Montgomery, and S. A. Braun, 2007: A Lagrangian trajectory view on transport and mixing processes between the eye, eyewall, and environment using a high-resolution simulation of Hurricane Bonnie (1998). *J. Atmos. Sci.*, **64**, 1835–1856, doi:10.1175/JAS3921.1.

Davis, C., and Coauthor, 2008: Prediction of landfalling hurricanes with the Advanced Hurricane WRF Model. *Mon. Wea. Rev.*, **136**, 1990–2005, doi:10.1175/2007MWR2085.1.

Doyle, J. D., and Coauthors, 2014: Tropical cyclone prediction using COAMPS-TC. *Oceanography*, **27** (3), 104–115, doi:10.5670/oceanog.2014.72.

Elsberry, R. L., 2002: Predicting hurricane landfall precipitation: Optimistic and pessimistic views from the symposium on precipitation extremes. *Bull. Amer. Meteor. Soc.*, **83**, 1333–1339, doi:10.1175/1520-0477(2002)083<1333:PHLPOA>2.3.CO;2.

Emanuel, K. A., 1995: Sensitivity of tropical cyclones to surface exchange coefficients and a revised steady-state model incorporating eye dynamics. *J. Atmos. Sci.*, **52**, 3969–3976, doi:10.1175/1520-0469(1995)052<3969:SOTCTS>2.0.CO;2.

Farfán, L. M., and J. A. Zehnder, 2001: An analysis of the landfall of Hurricane Nora (1997). *Mon. Wea. Rev.*, **129**, 2073–2088, doi:10.1175/1520-0493(2001)129<2073:AAOTLO>2.0.CO;2.

Gopalakrishnan, S. G., F. Marks, J. A. Zhang, X. Zhang, J. W. Bao, and V. Tallapragada, 2013: A study of the impacts of vertical diffusion on the structure and intensity of the tropical cyclones using the high-resolution HWRF system. *J. Atmos. Sci.*, **70**, 524–541, doi:10.1175/JAS-D-11-0340.1.

Hong, S. Y., and H. L. Pan, 1996: Nonlocal boundary layer vertical diffusion in a medium-range forecast model. *Mon. Wea. Rev.*, **124**, 2322–2339, doi:10.1175/1520-0493(1996)124<2322:NBLVDI>2.0.CO;2.

——, Y. Noh, and J. Dudhia, 2006: A new vertical diffusion package with an explicit treatment of entrainment processes. *Mon. Wea. Rev.*, **134**, 2318–2341, doi:10.1175/MWR3199.1.

Hou, D., and Coauthors, 2014: Climatology-calibrated precipitation analysis at fine scales: Statistical adjustment of stage IV toward CPC gauge-based analysis. *J. Hydrometeor.*, **15**, 2542–2557, doi:10.1175/JHM-D-11-0140.1.

Houze, R. A., and Coauthors, 2006: The Hurricane Rainband and Intensity Change Experiment: Observations and modeling of Hurricanes Katrina, Ophelia, and Rita. *Bull. Amer. Meteor. Soc.*, **87**, 1503–1521, doi:10.1175/BAMS-87-11-1503.

Janjić, Z. I., R. Gall, and M. E. Pyle, 2010: Scientific documentation for the NMM solver. NCAR Tech. Note NCAR/TN–477+STR, 53 pp., doi:10.5065/D6MW2F3Z.

Kaplan, J., and M. DeMaria, 2001: On the decay of tropical cyclone winds after landfall in the New England area. *J. Appl. Meteor.*, **40**, 280–286, doi:10.1175/1520-0450(2001)040<0280:OTDOTC>2.0.CO;2.

Kepert, J. D., 2001: The dynamics of boundary layer jets within the tropical cyclone core. Part I: Linear theory. *J. Atmos. Sci.*, **58**, 2469–2484, doi:10.1175/1520-0469(2001)058<2469:TDOBLJ>2.0.CO;2.

——, 2012: Choosing a boundary layer parameterization for tropical cyclone modeling. *Mon. Wea. Rev.*, **140**, 1427–1445, doi:10.1175/MWR-D-11-00217.1.

Kimball, S. K., 2006: A modeling study of hurricane landfall in a dry environment. *Mon. Wea. Rev.*, **134**, 1901–1918, doi:10.1175/MWR3155.1.

Knabb, R. D., J. R. Rhome, and D. P. Brown, 2005: Tropical cyclone report: Hurricane Katrina, 23–30 August 2005. NOAA/National Hurricane Center Rep., 43 pp. [Available online at http://www.nhc.noaa.gov/data/tcr/AL122005_Katrina.pdf.]

——, ——, and ——, 2006: Tropical cyclone report: Hurricane Rita, 18–26 September 2005. NOAA/National Hurricane Center Rep., 33 pp.

Kurihara, Y., and R. E. Tuleya, 1974: Structure of a tropical cyclone developed in a three-dimensional numerical simulation model. *J. Atmos. Sci.*, **31**, 893–919, doi:10.1175/1520-0469(1974)031<0893:SOATCD>2.0.CO;2.

Li, X., and Z. Pu, 2008: Sensitivity of numerical simulation of early rapid intensification of Hurricane Emily (2005) to cloud microphysical and planetary boundary layer parameterizations. *Mon. Wea. Rev.*, **136**, 4819–4838, doi:10.1175/2008MWR2366.1.

Liu, Q., N. Surgi, S. Lord, W. S. Wu, S. Parrish, S. Gopalakrishnan, J. Waldrop, and J. Gamache, 2006: Hurricane initialization in HWRF Model. *27th Conf. on Hurricanes and Tropical Meteorology*, Monterey, CA, Amer. Meteor. Soc., 8A.2. [Available online at https://ams.confex.com/ams/pdfpapers/108496.pdf.]

Marks, F. D., and L. K. Shay, 1998: Landfalling tropical cyclones: Forecast problems and associated research opportunities. *Bull. Amer. Meteor. Soc.*, **79**, 305–323, doi:10.1175/1520-0477(1998)079<0305:LTCFPA>2.0.CO;2.

Mellor, G. L., 2004: Users guide for a three-dimensional, primitive equation, numerical ocean model. Program in Atmospheric and Oceanic Sciences, Princeton University Rep., 56 pp.

Miller, B. I., 1964: A study on the filling of Hurricane Donna (1960) over land. *Mon. Wea. Rev.*, **92**, 389–406, doi:10.1175/1520-0493(1964)092<0389:ASOTFO>2.3.CO;2.

Nicholls, S., 1985: Aircraft observations of the Ekman layer during the Joint Air–Sea Interaction Experiment. *Quart. J. Roy. Meteor. Soc.*, **111**, 391–426, doi:10.1002/qj.49711146807.

Noh, Y., W. G. Cheon, S. Y. Hong, and S. Raasch, 2003: Improvement of the K-profile model for the planetary boundary layer based on large eddy simulation data. *Bound.-Layer Meteor.*, **107**, 401–427, doi:10.1023/A:1022146015946.

Nolan, D. S., J. A. Zhang, and D. P. Stern, 2009a: Evaluation of planetary boundary layer parameterizations in tropical cyclones by comparison of in situ data and high-resolution simulations of Hurricane Isabel (2003). Part I: Initialization, maximum winds, and outer core boundary layer structure. *Mon. Wea. Rev.*, **137**, 3651–3674, doi:10.1175/2009MWR2785.1.

——, D. P. Stern, and J. A. Zhang, 2009b: Evaluation of planetary boundary layer parameterizations in tropical cyclones by comparison of in situ observations and high-resolution simulations of Hurricane Isabel (2003). Part II: Inner-core boundary layer and eyewall structure. *Mon. Wea. Rev.*, **137**, 3675–3698, doi:10.1175/2009MWR2786.1.

Parrish, J. R., R. W. Burpee, F. D. Marks, and R. Grebe, 1982: Rainfall patterns observed by digitized radar during the landfall of Hurricane Frederic (1979). *Mon. Wea. Rev.*, **110**, 1933–1944, doi:10.1175/1520-0493(1982)110<1933:RPOBDR>2.0.CO;2.

Powell, M. D., 1982: The transition of the Hurricane Frederic boundary layer wind fields from the open Gulf of Mexico to landfall. *Mon. Wea. Rev.*, **110**, 1912–1932, doi:10.1175/1520-0493(1982)110<1912:TTOTHF>2.0.CO;2.

——, 1987: Changes in the low-level kinematic and thermodynamic structure of Hurricane Alicia (1983) at landfall. *Mon. Wea. Rev.*, **115**, 75–99, doi:10.1175/1520-0493(1987)115<0075:CITLLK>2.0.CO;2.

——, 1990: Boundary layer structure and dynamics in outer hurricane rainbands. Part II: Downdraft modification and mixed layer recovery. *Mon. Wea. Rev.*, **118**, 918–938, doi:10.1175/1520-0493(1990)118<0918:BLSADI>2.0.CO;2.

——, and S. H. Houston, 1996: Hurricane Andrew's landfall in south Florida. Part II: Surface wind fields and potential real-time applications. *Wea. Forecasting*, **11**, 329–349, doi:10.1175/1520-0434(1996)011<0329:HALISF>2.0.CO;2.

Pu, Z., X. Li, and J. Sun, 2009: Impact of airborne Doppler radar data assimilation on the numerical simulation of intensity changes of Hurricane Dennis near a landfall. *J. Atmos. Sci.*, **66**, 3351–3365, doi:10.1175/2009JAS3121.1.

Riemer, M., M. T. Montgomery, and M. E. Nicholls, 2010: A new paradigm for intensity modification of tropical cyclones: Thermodynamic impact of vertical wind shear on the inflow layer. *Atmos. Chem. Phys.*, **10**, 3163–3188, doi:10.5194/acp-10-3163-2010.

Rosenthal, S. L., 1971: The response of a tropical cyclone model to variations in boundary layer parameters, initial conditions, lateral boundary conditions, and domain size. *Mon. Wea. Rev.*, **99**, 767–777, doi:10.1175/1520-0493(1971)099<0767:TROATC>2.3.CO;2.

Shapiro, L. J., and H. E. Willoughby, 1982: The response of balanced hurricanes to local sources of heat and momentum. *J. Atmos. Sci.*, **39**, 378–394, doi:10.1175/1520-0469(1982)039<0378:TROBHT>2.0.CO;2.

Shelton, K. L., and J. Molinari, 2009: Life of a six-hour hurricane. *Mon. Wea. Rev.*, **137**, 51–67, doi:10.1175/2008MWR2472.1.

Sirutis, J. J., and K. Miyakoda, 1990: Subgrid scale physics in 1-month forecasts. Part I: Experiment with four parameterization packages. *Mon. Wea. Rev.*, **118**, 1043–1064, doi:10.1175/1520-0493(1990)118<1043:SSPIMF>2.0.CO;2.

Skamarock, W. C., and Coauthors, 2008: A description of the Advanced Research WRF version 3. NCAR Tech. Note NCAR/TN-475+STR, 113 pp., doi:10.5065/D68S4MVH.

Smith, R. K., 2003: A simple model of the hurricane boundary layer. *Quart. J. Roy. Meteor. Soc.*, **129**, 1007–1027, doi:10.1256/qj.01.197.

Stull, R. B., 1988: *An Introduction to Boundary Layer Meteorology*. Atmospheric and Oceanographic Sciences Library, Vol. 13, Kluwer Academic Publishers, 670 pp., doi:10.1007/978-94-009-3027-8.

Tallapragada, V., and Coauthors, 1986: A simple model of the atmospheric boundary layer; sensitivity to surface evaporation. *Bound.-Layer Meteor.*, **37**, 129–148, doi:10.1007/BF00122760.

——, and Coauthors, 2014: Hurricane Weather Research and Forecasting (HWRF) Model: 2014 scientific documentation. Developmental Testbed Center Tech. Rep., 105 pp.

Troen, I. B., and L. Mahrt, 1986: A simple model of the atmospheric boundary layer: Sensitivity to surface evaporation. *Bound.-Layer Meteor.*, **37**, 129–148, doi:10.1007/BF00122760.

Tuleya, R. E., and Y. Kurihara, 1978: A numerical simulation of the landfall of tropical cyclones. *J. Atmos. Sci.*, **35**, 242–257, doi:10.1175/1520-0469(1978)035<0242:ANSOTL>2.0.CO;2.

Whitehead, J. C., 2003: One million dollars per mile? The opportunity costs of hurricane evacuation. *Ocean Coastal Manage.*, **46**, 1069–1083, doi:10.1016/j.ocecoaman.2003.11.001.

Wilks, D. S., 1995: *Statistical Methods in Atmospheric Sciences: An Introduction*. Academic Press, 467 pp.

Willoughby, H. E., F. D. Marks, and R. J. Feinberg, 1984: Stationary and propagating convective bands in asymmetric hurricanes. *J. Atmos. Sci.*, **41**, 3189–3211, doi:10.1175/1520-0469(1984)041<3189:SAMCBI>2.0.CO;2.

Wu, C. C., and Y. H. Kuo, 1999: Typhoon affecting Taiwan: Current understanding and future challenges. *Bull. Amer. Meteor. Soc.*, **80**, 67–80, doi:10.1175/1520-0477(1999)080<0067:TATCUA>2.0.CO;2.

——, T. H. Yen, Y. H. Huang, C. K. Yu, and S. G. Chen, 2016: Statistical characteristic of heavy rainfall associated with typhoon near Taiwan based on high-density automatic rain gauge data. *Bull. Amer. Meteor. Soc.*, **97**, 1363–1375, doi:10.1175/BAMS-D-15-00076.1.

Zhang, J. A., and W. M. Drennan, 2012: An observational study of vertical eddy diffusivity in the hurricane boundary layer. *J. Atmos. Sci.*, **69**, 3223–3236, doi:10.1175/JAS-D-11-0348.1.

——, ——, P. G. Black, and J. R. French, 2009: Turbulence structure of the hurricane boundary layer between the outer rainbands. *J. Atmos. Sci.*, **66**, 2455–2467, doi:10.1175/2009JAS2954.1.

——, F. D. Marks, M. T. Montgomery, and S. Lorsolo, 2011: An estimation of turbulent characteristics in the low-level region of intense Hurricanes Allen (1980) and Hugo (1989). *Mon. Wea. Rev.*, **139**, 1447–1462, doi:10.1175/2010MWR3435.1.

——, S. Gopalakrishnan, F. Marks, R. F. Rogers, and V. Tallapragada, 2012: A developmental framework for improving hurricane model physical parameterizations using aircraft observations. *Trop. Cyclone Res. Rev.*, **1**, 419–429, doi:10.6057/2012TCRR04.01.

——, R. F. Rogers, P. D. Reasor, E. W. Uhlhorn, and F. D. Marks, 2013: Asymmetric hurricane boundary layer structure from dropsonde composites in relation to the environmental vertical wind shear. *Mon. Wea. Rev.*, **141**, 3968–3984, doi:10.1175/MWR-D-12-00335.1.

——, D. S. Nolan, R. F. Rogers, and V. Tallapragada, 2015: Evaluating the impact of improvements in the boundary layer parameterization on hurricane intensity and structure forecasts in HWRF. *Mon. Wea. Rev.*, **143**, 3136–3155, doi:10.1175/MWR-D-14-00339.1.

Zhu, P., 2008: Impact of land surface roughness on surface winds during hurricane landfall. *Quart. J. Roy. Meteor. Soc.*, **134**, 1051–1057, doi:10.1002/qj.265.

——, and J. Furst, 2013: On the parameterization of surface momentum transport via drag coefficient in low wind conditions. *Geophys. Res. Lett.*, **40**, 2824–2828, doi:10.1002/grl.50518.

——, K. Menelaou, and Z. D. Zhu, 2014: Impact of subgrid-scale vertical turbulent mixing on eyewall asymmetric structures and mesovortices of hurricanes. *Quart. J. Roy. Meteor. Soc.*, **140**, 416–438, doi:10.1002/qj.2147.